Synthesis, Characterization and Reactivity of Tungsten Oxynitride

by

Toby E. Lucy

Thesis submitted to the Faculty of the

Virginia Polytechnic Institute and State University

in partial fulfillment of the requirements for the degree of

MASTER OF SCIENCE

IN

CHEMICAL ENGINEERING

APPROVED:

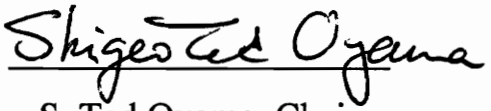

S. Ted Oyama, Chair

David F. Cox

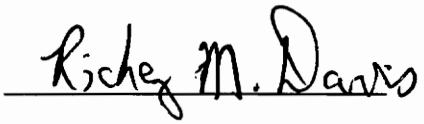

Richey M. Davis

August 30, 1996

Blacksburg, Virginia

Keywords: Tungsten Nitride, Catalysis, Synthesis, Reactivity, TPR

Synthesis, Characterization and Reactivity of Tungsten Oxynitride

by

Toby E. Lucy

S. Ted Oyama, Chairman

Department of Chemical Engineering

(ABSTRACT)

High surface area tungsten oxynitride samples have been prepared by the temperature programmed reaction (TPR) of WO_3 with NH_3. All samples were characterized by X-ray diffraction (XRD), nitrogen physisorption, and CO chemisorption. In addition, some sample compositions were determined by elemental analysis. Samples were prepared at various heating rates (β), allowing a Redhead analysis to be carried out giving an activation energy of nitridation of 109 kJ mol^{-1}. A heating rate of 0.016 K s^{-1} gave optimum synthesis conditions. Solid state intermediates were studied by interruption of the temperature program at various stages. No distinct suboxide phases formed along the synthesis path were found using XRD. An increase in surface area, CO uptake and nitrogen weight content, were found to occur as the reaction progressed. Reactivity experiments showed reasonable hydrodeoxygenation (HDO) and hydrodenitrogenation (HDN) activities, but little hydrogenation (HYD) or hydrodesulfurization (HDS) activities.

Acknowledgments

First I would like to thank Dr. S. Ted Oyama, Dr. David F. Cox, and Dr. Richey M. Davis the members of my M.S. committee for their suggestions and guidance.

I would like to especially thank Dr. Oyama, Todd St. Clair, Bala Dhandapani, Viviane Schwartz, and Todd Solberg for their various contributions to this work. Dr. Oyama has achieved much in the field of catalysis, and it was he who first suggested a study on tungsten nitride. He has also been a very personable advisor who enjoys spending time on social outings with the members of his lab. Todd was very helpful in bringing about a better understanding of the techniques used in this study with his own personal experience, and Bala in large part carried out the reactivity experiments that are mentioned in this report. They were also both friends whom I will miss when I leave Virginia Tech. Viviane Schwartz performed the elemental analysis for nitrogen content on the samples, and Todd Solberg was helpful in XRD matters. A great deal of assistance was also given by Rajat Kapoor, Wei Li, and Sasangan Ramanathan who helped discuss the experimental results with me which aided in my understanding of the work I was conducting.

I would also like to thank the members of my family, especially my parents Melvin and Bonnie Lucy, who besides contributing financially to my education also provided emotional support during my time in Blacksburg. It is my hope that the work that I have completed here at Virginia Tech will make them proud of me.

Last, but certainly not least, I would also like to mention: Anil Prabhu, Viviane Schwartz, Weimin Zhang, Paul Clark, Rakesh Radhakrishnan, Jill Restad, Fred Gibson, Mark Abee, Steve York, Tara and Slade Gardner, Norman Broyles, Phil Kaiser, Fanny Schwagert, and James Mann, to thank them for their friendship in my time in the Chemical Engineering Department at Virginia Tech. I wish all of those that I have mentioned, the best in their future and their careers.

Table of Contents

1. Introduction 1
2. Literature Review 4
   2.1 Synthesis 4
      2.1.1 Low surface area materials 4
      2.1.2 High surface area materials 5
      2.1.3 Films and Coatings 7
   2.2 Reactivity 9
   2.3 Objectives 10
3. Experimental 11
   3.1 Synthesis 11
   3.2 Characterization 15
   3.3 Reactivity 16
4. Results and Discussion 19
   4.1 Synthesis 20
   4.2 Characterization 27
   4.3 Reactivity 37
5. Conclusions 42
6. Appendix 44
7. References 50

1. Introduction

Transition metal carbides and nitrides are a unique class of compounds that combine properties of both ceramics and metals. They are found over wide ranges of stoichiometry, and have very high melting points (>3300 K) and hardness values (>2000 kg mm^{-2}) that fall in the range of ceramics. In addition, their electrical and magnetic properties include Hall coefficients and electrical conductivities that are in the range of metals[1]. The industrial uses of these materials are numerous, and include coatings on cutting tools and diffusion barriers in semiconductor contacting technology[2].

In carbides and nitrides, the non-metal atoms occupy interstitial sites in the metal lattice, typically octahedral in both face-centered cubic (fcc) and hexagonal close packed (hcp) structures, and trigonal prismatic sites in simple hexagonal structures. The formation of carbides and nitrides usually results in a crystal structure different than that of the parent metal. The particular type of crystal structure that is formed is governed by two factors: geometric and electronic[3]. The geometric factor follows an empirical rule by Hägg which states that simple structures are formed when the hard ball radii of non-metal to metal is less than 0.59[4]. The electronic factor is based on the Engel-Brewer theory of metals which states that as *s-p* electron count is increased, the crystal structure will shift from body-centered cubic (bcc) to hcp to fcc[5]. For instance, Group 6 metals (W, Mo) are bcc, Group 7 metals (Tc, Re) are hcp, and Group 10 metals (Pd, Pt) are fcc. In an analogous manner, W metal is bcc, β–W_2C is hcp, and β-W_2N is fcc, indicating an increase in the electron to metal ratio. The number of valence electrons increases as one

proceeds from C to N and hence the crystal structure also progresses from bcc to hcp and fcc[3]. This serves as a possible explanation for the Pt-like behavior of carbides and nitrides by reasoning that as the electron count increases, the Group 6 carbides and nitrides become like the Group 10 metals. This similarity between the catalytic properties of Pt and transition metal carbides and nitrides has sparked interest in developing an inexpensive alternative to the widely-used noble metal catalysts.

To develop the carbides and nitrides as catalysts, a synthesis method is desired which results in high surface area materials. Traditional powder metallurgy results in very low surface areas because of the high temperatures employed[6]. However, preparation of high surface area carbides and nitrides can be achieved using temperature programmed reaction (TPR) at lower temperatures[7]. The TPR method consists of heating an oxide precursor in a flow of CH_4/H_2 or NH_3 to obtain the carbide or nitride, respectively. Volpe and Boudart[8] first reported the synthesis of high surface area β-W_2N (91 $m^2\ g^{-1}$) using the TPR method. In this study, we report the preparation of a high surface area tungsten oxynitride at lower temperatures than previously reported. The materials have been characterized using x-ray diffraction (XRD), surface area measurements, CO chemisorption, and elemental analysis. The effect of heating rate on surface area and CO chemisorption has been investigated, and the activation energy for the nitridation step has been calculated. In addition, solid state intermediates for the transformation from WO_3 to oxynitride have been studied. The characterization led to an

optimized synthesis, yielding high site density tungsten oxynitride which was used in the activity studies.

The carbides and nitrides have excellent catalytic properties for reactions such as hydroprocessing[9], dehalogenation[10], and hydrogenation[11]. In particular, β-W_2N has been shown to be an effective catalyst for quinoline hydrodenitrogenation (HDN)[12], n-heptane isomerization[13], and alcohol dehydration[14]. In this study, we tested tungsten oxynitride for its hydrotreating HDN, HDS, HDO, and hydrogenation activities in a high pressure unit with feeds containing moderate amounts of S, N, O, and aromatics.

2. Literature Review

2.1 Synthesis

Carbides and nitrides have been prepared using different synthesis techniques. Oyama has summarized several general references on carbide / nitride synthesis[3]. Preparation methods are generally classified into three groups which depend upon the nature of the products. This section will provide an overview of the techniques used for each of the three types of materials.

2.1.1 Low surface area materials

Low surface area carbide / nitride products can be produced by a number of ways. A first such technique involves the reaction of the parent metal with solid carbon or molecular nitrogen. Thermodynamic calculations show that carbide formation is favorable here at low temperatures[15], however higher temperatures are used to counter solid-state diffusion barriers[16]. It has been previously demonstrated that N_2 does not react with or dissolve in metallic tungsten[17]. A reaction diagram showing the changes in free energy that occur in the formation of some of the Group 6A nitrides by the use of different techniques has been prepared by Lyutaya[18], and appears here in the appendix (Figure A1).

A number of other methods are used that form low surface area materials. One technique involves the reaction between the metal oxide powder and solid carbon with

heating. The reaction between the oxides and carbon are thermodynamically favored[16]. Carbide formation occurs either by reduction of the oxide to the parent metal followed by diffusion of carbon into the metal, or by the formation of a suboxide followed by carbon incorporation to form an oxycarbide. For carbothermal nitridation of oxides this is a common preparation method. A drawback of the technique is that it produces impure phases.

Low surface area carbides and nitrides can also be made by solid combustion synthesis. This method is commonly referred to as self-propagating high-temperature synthesis or SHS. The preparation involves the parent metal and a reactive gas, and continues spontaneously by the dissolution of carbon or nitrogen in the metals which is an exothermic process.

Single crystal samples can also be prepared. These allow for the examination of mechanical, electrical, and surface properties. Carbide single crystals are prepared by the Vernouil[1] technique, precipitation from liquid metals, and the floating zone technique. Nitrides are prepared by vapor transport methods.

2.1.2 **High surface area materials**

High surface area carbides and nitrides also can be prepared by a number of synthesis techniques. The reaction of a metal or metal oxide with a reactant gas is one example. This involves the use of isothermal conditions, and the reactant gas is carbon-containing for carbides, and usually NH_3 for nitrides. Ammonia is used rather than molecular nitrogen because it is a stronger nitriding agent. Kiessling and Peterson[19]

formed a tungsten oxynitride with a defective B1 (NaCl) structure in the WO_3 / NH_3 reaction at 973 K. In another study involving the WO_3 /NH_3 reaction , Lyutaya[18] formed the compound WO_2NH_2 with an unresolved structure below 873 K, and an oxynitride having an fcc crystal lattice at higher temperatures.

Two decomposition techniques are also in use for the formation of high surface area products. The first involves the use of the vapors of decomposed metal halides and gaseous hydrocarbons. This allows for the recovery of small amounts of pure carbides. The Van Arkel[20] process is used to make a number of nitrides. The use of H_2 and N_2 is often preferred over NH_3 here since ammonia decomposes at the high temperatures required for this method. Another decomposition technique involves using a laser as a heat source to react metal carbonyls with H_2 to form carbides and nitrides[21,22]. This technique promotes fast growth and rapid temperature changes (100 000 K s^{-1}) in the reaction zone. A structural characterization study of nanocrystalline β-W_2N prepared by this method is available[23].

Temperature programmed reaction (TPR) is still another method for preparing high surface area samples. This involves heating a precursor material in a reactive gas stream at a uniform rate. The precursor is usually an oxide, sulfide, nitride or other compound, and the reactive gases employed are usually CH_4 and H_2 for carbide formation, and NH_3 for nitride formation. The use of NH_3 is limited because it decomposes at >750 K. The precursor, usually a powder, is placed in a packed bed of a flow reactor. The outlet gas stream concentrations can be monitored allowing for the

determination of the completion of the product formation. In this method the metallic state can be bypassed and sintering of the samples can therefore be greatly reduced. This technique is particularly useful for the formation of samples with very high specific surface areas. Volpe and Boudart[8] were the first to effectively utilize this technique for the formation of high surface area β-W_2N from a WO_3 precursor.

High surface area supports can also give better control of surface area and pore size distribution. A highly dispersed carbide can be prepared by deposition of the precursor on the support followed by carburization. Lee[24], et al., for example prepared a molybdenum carbide supported on alumina.

Ultra-high surface area carbides have also been reported by the reaction between a metal oxide vapor and solid carbon. This process uses activated carbon, which acts as a support for the metal compound that is produced. Surface areas between 100 and 400 m^2 g^{-1} have been found for samples prepared in this manner.

2.1.3 **Films and Coatings**

The last class of carbides and nitrides consists of films and coatings. The various techniques used for their preparation include plasma synthesis, chemical vapor deposition (CVD), physical vapor deposition, and electrochemical reduction. These techniques have a variety of uses as will now be briefly explained.

The use of plasmas for synthesis allows for the deposition of a thin protective coating on metal surfaces. There are two plasma types currently in use in materials

processing[25]. The first is a thermal plasma, in which electrons are at comparable temperatures to the gas molecules. The temperatures of use are generally in the thousands of degrees. Glow discharge plasmas have electrons that are at higher temperatures than the gas molecules present. Reactive intermediates are formed through electron impact, and then cause gas-phase reactions. This plasma type is used for treating solid surfaces. Industrial uses include the coating of springs, camshafts, and forging dyes[26,27]. Lower temperatures can be used for nitriding samples allowing for better metallurgical control. Carbides results in better case uniformity allowing production of gears and other complex shapes.

Chemical vapor deposition allows for the formation of thin films or coatings to be placed on the surface of a substrate[28,29]. This process involves chemical reaction of gas phase species on to a heated substrate surface. The coatings formed are generally free of porosity and inclusions. The process is usually carried out at low pressure using gas phase inorganic metal halides, but also utilized are volatile metallic precursors containing C or N. The coatings are used in electronics manufacturing, tooling, fuel cogeneration, and in the aerospace industries[30]. A review summarizes the preparation of metals, borides, carbides, nitrides, oxides, and silicides[31]. A tungsten nitride thin film synthesis produced by reaction of WCl_6 with NH_3, H_2 and Ar has also been reported[32].

Physical vapor deposition differs from the CVD method in that there is an absence of surface reactions occurring that release byproducts that are not similar to the film composition. The physical deposition process can be thought of as surface condensation

of units having the same composition as the film. Sputtering or implantation methods can also be grouped along with this method. For instance, Bosseboeuf, et. al., have prepared tungsten nitride films by a reactive ion-beam sputter deposition[33].

A final film and coating technique involves the electrochemical reduction of metal oxides in carbonate melts. Studies have been conducted on the preparation of carbides, borides, and arsenides of Mo and W using this technique[34,35]. This study produced millimeter sized crystallites on the sides of a graphite crucible.

2.2 **Reactivity**

In recent years carbides and nitrides have been found to have excellent activity for various reactions involving hydrogen transfer. Studies concerning hydrodenitrogenation (HDN)[36,37,38], hydrodeoxygenation (HDO), hydrodesulfurization (HDS)[39,40], hydrogenation (HYD)[41,42], hydrogenolysis[43], and isomerization[44,45,46] of hydrocarbons by carbide and nitride catalysts appear often in the literature. Studies have also shown tungsten nitride to be an effective catalyst for quinoline hydrodenitrogenation (HDN)[12], n-heptane hydroisomerization[13], and alcohol dehydration[14].

The focus of the hydroprocessing reactivity experiment conducted on tungsten oxynitride that appears in this report follows the same procedure as that used by Ramanathan and Oyama[9] in their study of several carbide and nitride catalysts. Here, the catalysts were tested for HYD, HDN, HDS, and HDO activities using model liquid

compounds at 643 K and 3.1 MPa. A proposed reaction pathway for quinoline HDN that appears in that report has been reproduced here in the Appendix (Figure A2).

2.3 **Objectives**

The objectives of this study can be outlined as follows. First, to synthesize WO_xN_y from WO_3 by the TPR method. Then, to prepare oxynitride samples at different heating rates. Third, to characterize these samples and determine optimum synthesis conditions. Next, to interrupt an oxynitride synthesis at various stages and determine solid state intermediates by XRD. In addition, these interrupted synthesis samples will be characterized to determine any potential trends in the data. Finally, to test the reactivity of optimized WO_xN_y in a high-pressure reactor.

3. Experimental

3.1 Synthesis

The gases that were used in this study were NH_3 (LaRoche Anhydrous Premium Grade, 99.99%), He (Airco, 99.999%), 0.5% O_2/He (Airco UHP Grade), CO (Airco, 99.99%), H_2 (Airco, 99.999%), 30% N_2/He (Airco, 99.99%), 10% H_2/He (Airco, 99.99%), and N_2 (Airco, 99.99%). Alltech drierite filters with molecular sieves were used to purify each of the gases except NH_3, which utilized a KOH filter and a molecular sieve.

The precursors used to synthesize tungsten oxynitride were WO_3 (Johnson Matthey, 99.8%) and ammonium hydroxide (Fisher Scientific) the precursor. Other chemicals employed included: dibenzothiophene (Aldrich, 98%), quinoline (Aldrich, 98%), benzofuran (Aldrich, 99.5%), tetralin (Aldrich, 97%), tetradecane (Acros, 99%), cumene (Aldrich, 99%), and styrene (Aldrich 99%) which were used as received.

The reactor that was used in the synthesis of all the samples was a quartz U-tube of 15 mm O.D. that was placed in a furnace (Hoskins 550 W). The temperature of the furnace was controlled by a temperature programmer (Omega Model CN2000), and monitored by a chromel-alumel thermocouple that was placed in the thermocouple well located on the side of the reactor bed. The gases exiting the reactor were pumped into a mass spectrometer (Ametek / Dycor Model MA100) through a variable leak valve (Granville Phillips Model 203) by the use of a turbomolecular pump (Pfeiffer/Balzers TPU050). The mass spectroscopy and temperature data were recorded by a computer

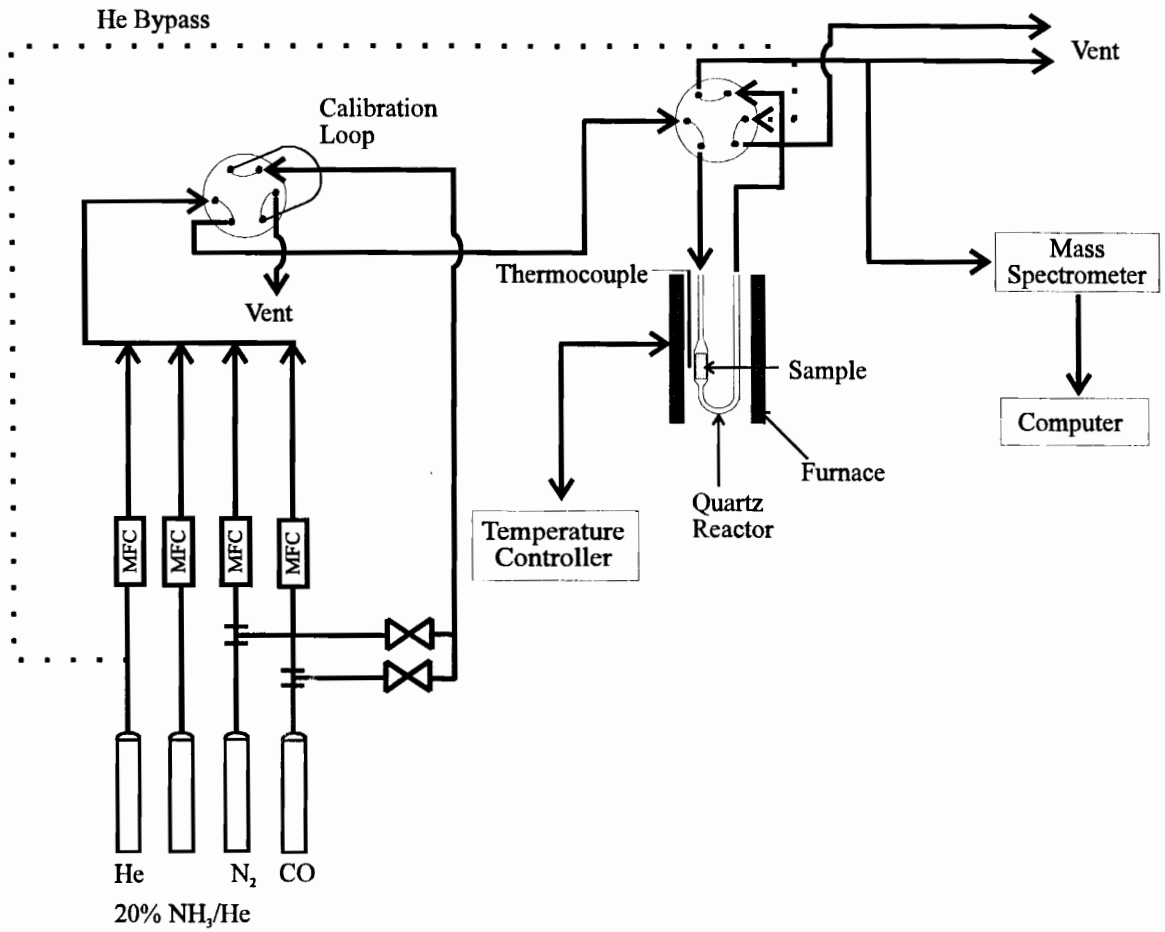

Figure 1: Schematic of Flow Reactor System.

(IBM PC compatible) through an RS232 interface. A schematic of the synthesis unit is presented in Figure 1.

The WO_3 powder precursor was determined to be too fine to remain within the reactor bed, so pellets were prepared by mixing the powder with ammonium hydroxide to form a slurry. The slurry was then slowly heated on a hot plate until the sample had hardened. The sample was then broken up and sieved through 16 and 20 mesh sieve trays to get pellets of around 1000 μm in diameter that would not pass through the reactor bed. About 1.0 g of WO_3 pellets were then placed in the reactor for all of the syntheses.

Tungsten oxynitride samples were prepared by temperature programmed reaction (TPR). The experimental procedure consisted of passing 136 μmol s^{-1} of NH_3 and 545 μmol s^{-1} of He over the precursor pellets while a temperature program was begun, the effluent gases being monitored by mass spectroscopy. The signals followed during synthesis included masses: 2, 4, 15, 17, 18, 28, 30, 44, and 46. The temperature program employed in this study consisted of two ramped stages of heating followed by a soak at constant temperature. The first stage raised the temperature quickly from ambient conditions to 673 K at a rate of 0.167 K s^{-1}. The heating ramp was then decreased to the desired rate until the maximum temperature used in the experiment was reached (T_{max}). Heating rates employed for this second stage were (0.067, 0.033, 0.017, and 0.008 K s^{-1}). The samples were then soaked at T_{max} in the reactant gases, for a length of time which usually lasted from about 0.5-1.0 h.

Soak times were dependent upon the disappearance of the mass 18 signal which indicated the cessation of water formation and the completion of the nitride synthesis. After soaking, the gas flow was switched to pure helium (30 μmol s^{-1}), and the temperature quickly reduced to ambient conditions. When the reactor reached room temperature, the flow was switched to a mixture of 100% He (0.833 cm^3 s^{-1}) and 0.5% O_2/He (0.833 cm^3 s^{-1}) for passivation. The flow of 100% He was gradually reduced over the course of about 0.5 h until only the 0.5% O_2/He remained flowing. This process prevented the introduction of too much O_2 initially, which would cause a sharp rise in temperature, and bulk oxidation of the sample. The 0.5% O_2/He flow was then continued for several hours, depositing a protective layer of oxygen on the surface of the fresh catalysts in order to prevent bulk oxidation upon removal from the reactor and exposure to air.

Initial syntheses of the nitride at different heating rates allowed for constant linear heating past the peak reaction temperature (T_p), so that a Redhead analysis[47] (Equation 1)

$$\ln\left(\frac{\beta}{T_p^{\,2}}\right) = C - \frac{E_a}{RT_p} \qquad (1)$$

could be used to determine the apparent activation energy of nitridation. Here, β represents the heating rate used (in K s^{-1}), T_p is the reaction rate maximum temperature (in K), E_a is the activation energy (in kJ mol^{-1}), and R is the universal gas constant. C is a constant which contains parameters for the solid, reaction order, and preexponential factor. The constant (C) will not be studied further in this report. T_p corresponded to the

maximum of the mass 18 (H_2O) desorption trace, and varied in a reproducible fashion according to the heating rate used. The analysis technique plots ln (β T_p^{-2}) against T_p^{-1}. Using linear regression, a slope is obtained which has a value of ($-E_a R^{-1}$).

3.2 **Characterization**

Nitrogen physisorption and CO chemisorption were measured with an automated system (Micromeritics ASAP 2000), which consisted of a sample preparation and analysis unit, and a computer interface. For physisorption, a 5-point BET analysis was conducted at liquid nitrogen temperature after degassing the sample at 723 K for 2 h. A single point physisorption method was also employed using the synthesis unit. Chemisorption of CO was also performed on the Micromeritics unit at 308 K after reduction of the sample in H_2 at 723 K for 2 h.

XRD analysis was carried out using a powder diffractometer (Scintag, Model ASC0007) with a CuKα monochromatized radiation source. The system was operated at 45kV and 40mA, slitwidths of 1.0 and 0.5 were used, a chopper increment of 0.15 and a scan rate of 1.0° 2θ min^{-1} . The XRD patterns were studied using the Scherrer[48] equation in order to determine the crystallite size of the oxynitride samples prepared (Equation 2).

$$D_c = \frac{K\lambda}{\beta \cos(\theta)} \qquad (2)$$

Here, (λ) is the wavelength of X-ray radiation, in nm, (β) is the peak width at half-maximum, in radians, (θ) is the Bragg angle, also in radians, and (K) is a constant usually taken to be 0.9. An instrumental line broadening must be subtracted from the value

obtained for the FWHM in order to obtain the true value of (β). The value of broadening used in this report is (0.1^0 θ). The method, as used here, focuses on the peak corresponding to the (1 1 1) plane of the oxynitride that occurs at about 37.6 ^{0} 2θ.
A qualitative elemental analysis was also carried out on two of the final product samples, the WO_3 powder, and a tungsten nitride standard (Pfaltz & Bauer 99.5%) in order to determine if oxygen was present in these samples. This analysis was carried out using an Electron Microprobe(CAMECA SX50). Quantitative values of nitrogen content in samples were determined by a Carlo Erba CHNS EA1108 Elemental Analyzer. Oxygen content in a sample was quantitatively determined through the use of the synthesis unit.

3.3 **Reactivity**

The reactivity of tungsten oxynitride was tested for hydrodenitrogenation (HDN), hydrodeoxygenation (HDO), hydrodesulfurization (HDS) and quinoline conversion activities in a high-pressure trickle-bed reactor operated at 3.1 MPa and 643 K. The feed consisted of 3000 ppm sulfur (dibenzothiophene), 2000 ppm nitrogen (quinoline), 500 ppm oxygen (benzofuran), 20 wt% aromatics (5 wt% amylbenzene and 15 wt% tetralin) and the balance was tetradecane. This mixture is typical of S, N, and O values found in liquid coal feeds. The catalyst (about 0.3 g) corresponding to 30 m^2 of overall surface area, was placed in a 316 SS tubular reactor which was immersed in a fluidized sand bath (Techne, Model SBL2) for good heat transfer. A detailed overview of the high-pressure

trickle-bed reactor system can be found elsewhere[9], but a schematic of the system is presented in Figure 2.

Hydrogen flow to the reactor was regulated by a mass flow controller (Brooks, Model 5850E). The liquid feed was introduced into the reactor with the use of high-pressure liquid pumps at a rate of 5 $cm^3 h^{-1}$. Before the catalyst was exposed to the liquid feed it was reduced in-situ in hydrogen at atmospheric pressure at 723 K for three hours. Following pretreatment, the reactor temperature was lowered to 643 K, the H_2 was pressurized to 3.1 MPa and the liquid feed was started. The liquid was also pressurized to 3.1 MPa before mixing with the H_2. The liquid and H_2 flowed upwards through the catalyst bed and then out of the reactor to a liquid sampling valve. Liquid samples were collected at regular intervals for a period of 60 h at which time it was determined that the various activities had reached steady state conversion. The samples were analyzed off-line using a gas chromatograph (HP 5890 Series II) equipped with a capillary column (CPSIL-5CB, Chrompack, Inc.) and flame ionization detector. At the end of the reaction, the catalyst was washed in hexane to remove residual reactant from the surface and then stored for post-reaction characterization using XRD.

In a second reactivity experiment the oxynitride was tested for the hydrogenation of cumene. In this study the reactant was cumene (5 wt. %), and the balance was tetradecane. The catalyst was tested using a similar procedure as that described previously for the hydrotreatment experiment. For this study amounts of catalyst were

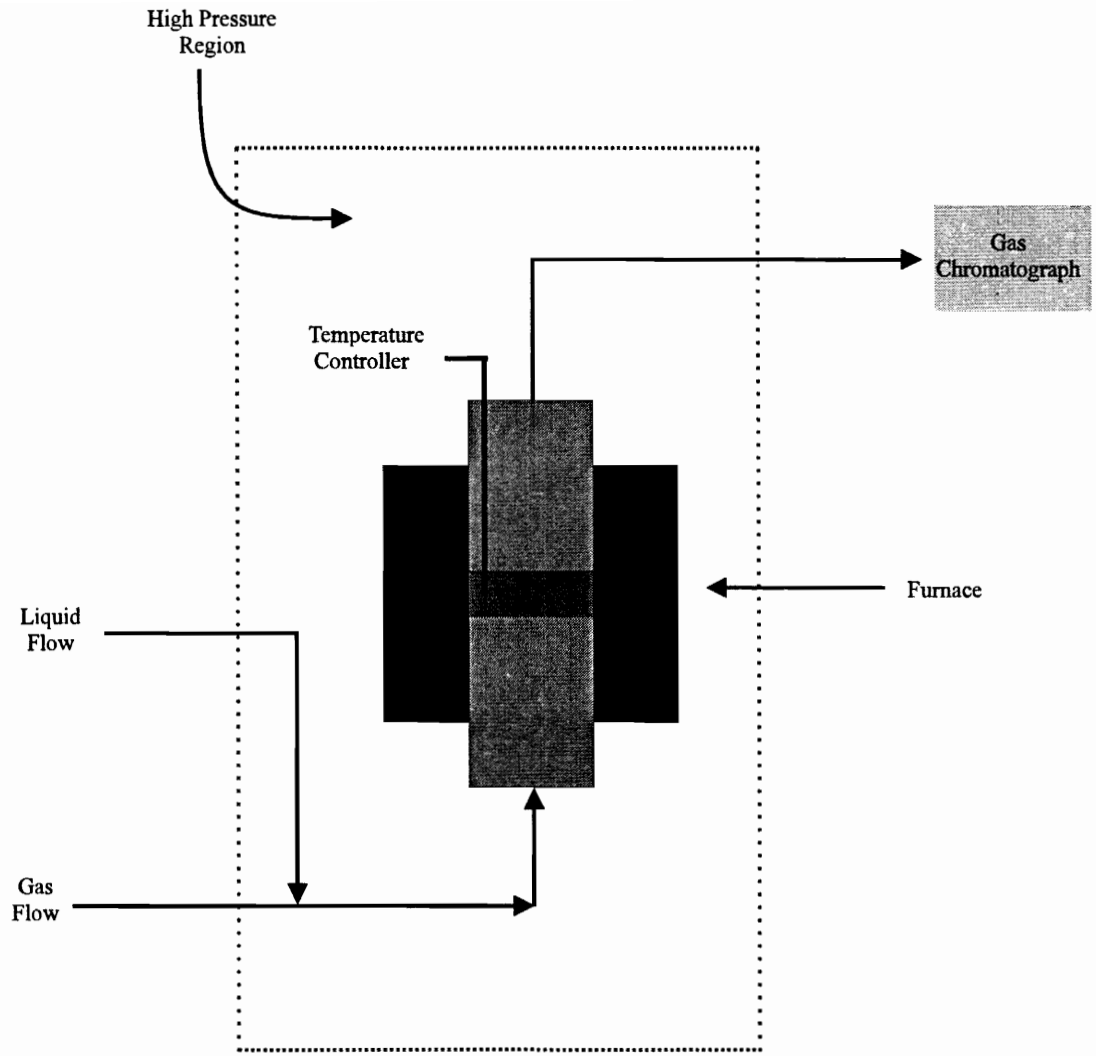

Figure 2: Schematic of Trickle-Bed Reactor System Diagram

loaded equivalent to 70 μmol of irreversible CO uptake. This corresponded to about 0.5 g of sample. The catalyst was then activated in H_2 at atmospheric pressure and 723 K for 2.0 h. After cooling to 523 K, the system pressure was raised to 5.1 MPa of H_2, and the liquid feed was introduced into the reactor at a rate of 5 $cm^3 h^{-1}$. The liquid effluent from the reactor was then analyzed off-line using gas chromatography in the same manner as before. After completion of the experiment, the catalyst was washed in hexane to remove any residual liquid from the surface. The spent catalyst was then characterized using XRD.

In a third reactivity experiment, the activity of styrene hydrogenation was studied. The experimental setup here was the same as in the case of cumene hydrogenation with the following exceptions. The amount of styrene in the feed was (5 wt. %) and the balance tetradecane. Also 100 ppm of dibenzothiophene was added to the feed after 50 h on line. The amount of catalyst loading was again for 70 μmol of irreversible CO uptake, however this was a sample with a lower CO uptake requiring the loading of 0.8 g.

4. Results and Discussion

4.1 Synthesis

There appears to be a relatively small body of work in the past concerning the synthesis of tungsten nitride . Kiessling and Peterson[19] formed a tungsten oxynitride with a defective B1 (NaCl) structure during the WO_3 / NH_3 reaction at 973 K. In another study involving the WO_3 /NH_3 reaction , Lyutaya[18] formed the compound WO_2NH_2 with an unresolved structure below 873 K, and an oxynitride having an fcc crystal lattice at higher temperatures. This work also showed that to fully remove the oxygen from the sample, prolonged heating for 2 h at 1173 K was required. However, this high temperature also caused the removal of almost all of the nitrogen from the sample leaving almost pure tungsten metal. Lyutaya then developed a two-stage synthesis process in which WO_3 was reduced and nitrided in a fast stream of NH_3 at 1173 K, followed by a reduction in temperature to 873 K to obtain a pure phase of β-W_2N. No data concerning physisorption and chemisorption of the prepared sample was given in either of these two papers.

A previous synthesis of high surface area tungsten nitride by the TPR method was carried out by Volpe and Boudart[8]. In that study, molar flow rates of 70-100 μmol s^{-1} NH_3 were passed over packed beds of 0.2-1.0 g of WO_3 precursor (giving molar space velocities with a range of 0.02-0.08 s^{-1}) and heated at 0.01 K s^{-1} to a final temperature of 1025 K. These synthesis conditions produced β-W_2N samples with S_g as high as 91

$m^2\ g^{-1}$, and CO uptakes as high as 200 μmol g^{-1}.

In the current study, a series of tungsten oxynitride samples were prepared following a procedure similar to that outlined by Volpe and Boudart. However, the samples were formed at a lower temperature (923 K) than reported in that study, but at a much larger NH_3 flow rate of 680 μmol s^{-1} (corresponding to a molar space velocity of 0.16 s^{-1}). At higher temperatures than 923 K, a W metal phase began to form and increase in comparison to the oxynitride phase, until at 1123 K the sample was essentially all metal. The XRD patterns from these initial syntheses are presented in Figure 3.

The concentration of NH_3 used in the initial syntheses was determined to be too large to allow accurate monitoring of the mass 18 (H_2O) trace, as this mass signal was being overwhelmed by the mass 17 (NH_3) signal. A mixture of 20% NH_3/He was therefore used, maintaining the same space velocity of the initial syntheses runs. This corresponded to molar flow rates of 136 μmol s^{-1} NH_3 and 545 μmol s^{-1} He. This mixture was used in all of the subsequent syntheses. A representative synthesis plot showing the mass signals followed and a typical temperature program employed appears in Figure A3 of the Appendix.

Next, tungsten oxynitride samples synthesized at various heating rates (β) were prepared. The heating rates used ranged from 0.008 to 0.067 K s^{-1}. The results of this study showed that at lower values of β, the maximum rate of reaction, found by monitoring the mass 18 signal, occurred at lower peak temperatures (T_p). A Redhead analysis (Equation 1) was employed, using the β and associated T_p values, in order to

determine the apparent activation energy of nitridation. The Redhead analysis results are plotted in Figure 4. From this, an activation energy of 109 kJ mol^{-1} was determined. In comparison, Lyutaya[18] determined β-W_2N and oxynitride formation activation energies to be 157 kJ mol^{-1} and 136 kJ mol^{-1} respectively. The discrepancy could possibly be due to their use of lower flow rates, which would result in interference from the reverse reaction. Lyutaya employed isothermal heating of the samples which might also cause a difference. In another study, a series of oxynitride syntheses were carried out to investigate the nature of solid state intermediates formed during the reaction. The TPR mass spectroscopy traces show four distinct mass 18 (H_2O) peaks which follow the course of the formation of the nitride. A mass spectroscopy trace of mass 18 against reaction temperature for a typical synthesis using a 0.033 K s^{-1} heating rate is presented in Figure 5.

During the initial temperature ramp of 0.167 K s^{-1} from room temperature to 673 K, the first three mass 18 peaks occurred at 400, 560, and 670 K. The final peak occurred at different temperatures depending on the heating rate used for the final ramp. These temperatures are listed in Table 1. In some of the syntheses, mass 30 (NO) and, much less often, mass 44 (N_2O) peaks were observed to occur at the same temperatures as the mass 18 peaks. The exception was the mass 18 peak at 670 K, which did not show any sign of mass 30 or mass 44 desorption. No other masses monitored showed distinguishing peaks requiring any further investigation. The first step in the identification of possible solid state intermediates was to determine the composition

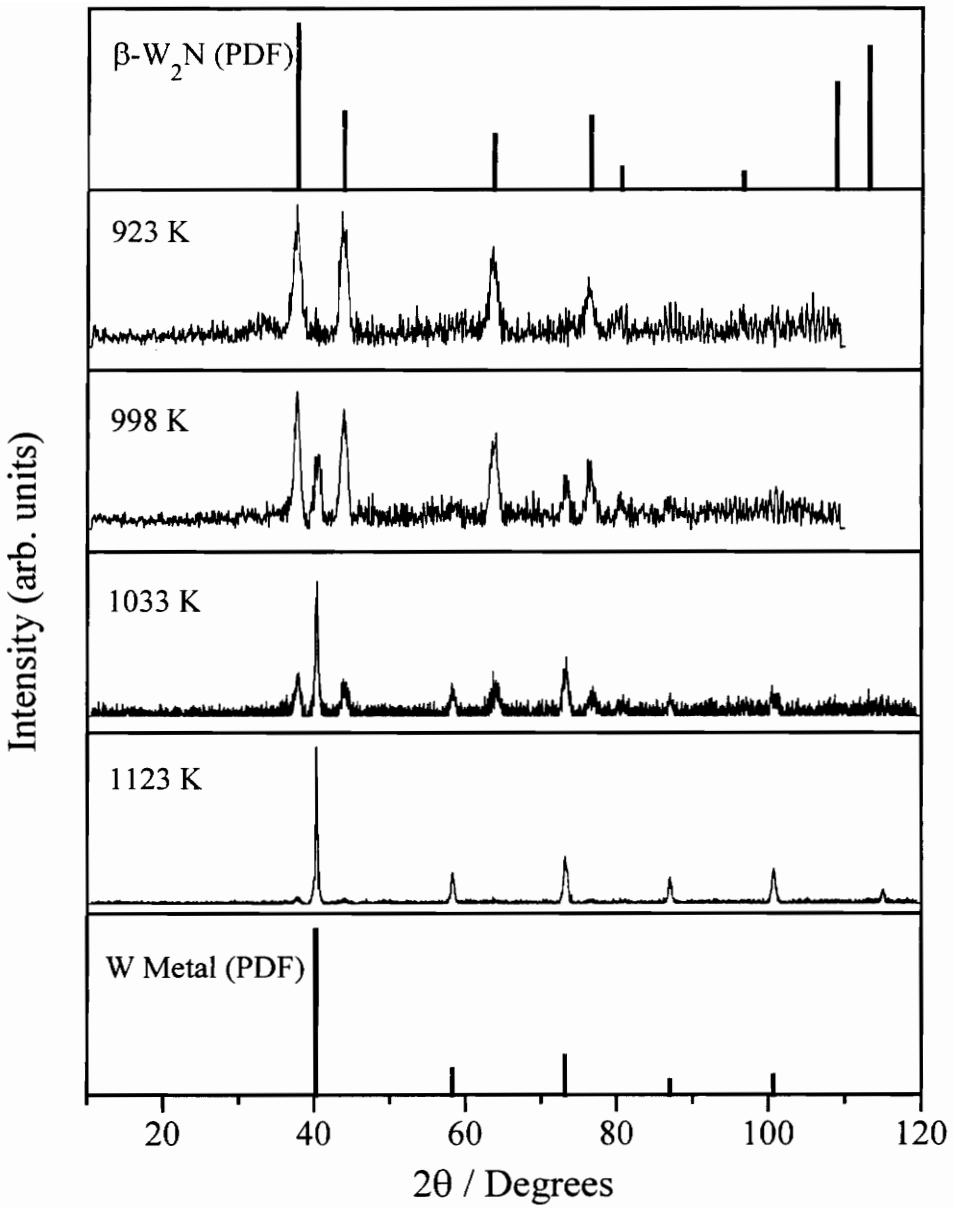

Figure 3: XRD Patterns from Initial Syntheses of Tungsten Oxynitride. Powder diffraction file data on β-W_2N and W metal are included to show the progression of W metal formation.

formed with each of the first three mass 18 peaks. As was mentioned briefly in the experimental section, the precursor pellets used were actually a two phase solid mixture of WO_3 and $(NH_4)_{10}W_{12}O_{41}$ as determined by XRD (Figure 6, pattern (a)). Three identical syntheses were conducted in which the heating was interrupted after each peak had come back to baseline. The interruption points for the three experiments are given in Figure 5 (stages b-d). The identity of these samples will be discussed in the characterization section. The second stage of solid state intermediate analysis concerned the higher temperature mass 18 peak which occurred at different temperatures depending upon the heating rate used, indicating the formation of the nitride. The trace shows only this single mass 18 peak, with no distinct features which could be associated with intermediate stages forming during synthesis. In the formation of VN, for example, Kapoor and Oyama[49] found several small peaks in the mass 28 signal as well as one in the mass 2 signal indicating the formation of solid state intermediates. A mass 30 peak was also observed to occur simultaneously with the mass 18 peak, but again showed no distinct features. For this reason, several experiments were carried out in which the reaction was interrupted at various stages (intermediate temperatures) along the mass 18 peak using a heating rate for each of 0.033 K s^{-1}. After heating to the temperatures indicated for each interruption, the samples were soaked in the reactant gases at temperature, until the mass 18 signal returned to baseline which usually took about 0.5 h. The identity of these samples will also be discussed in the characterization section.

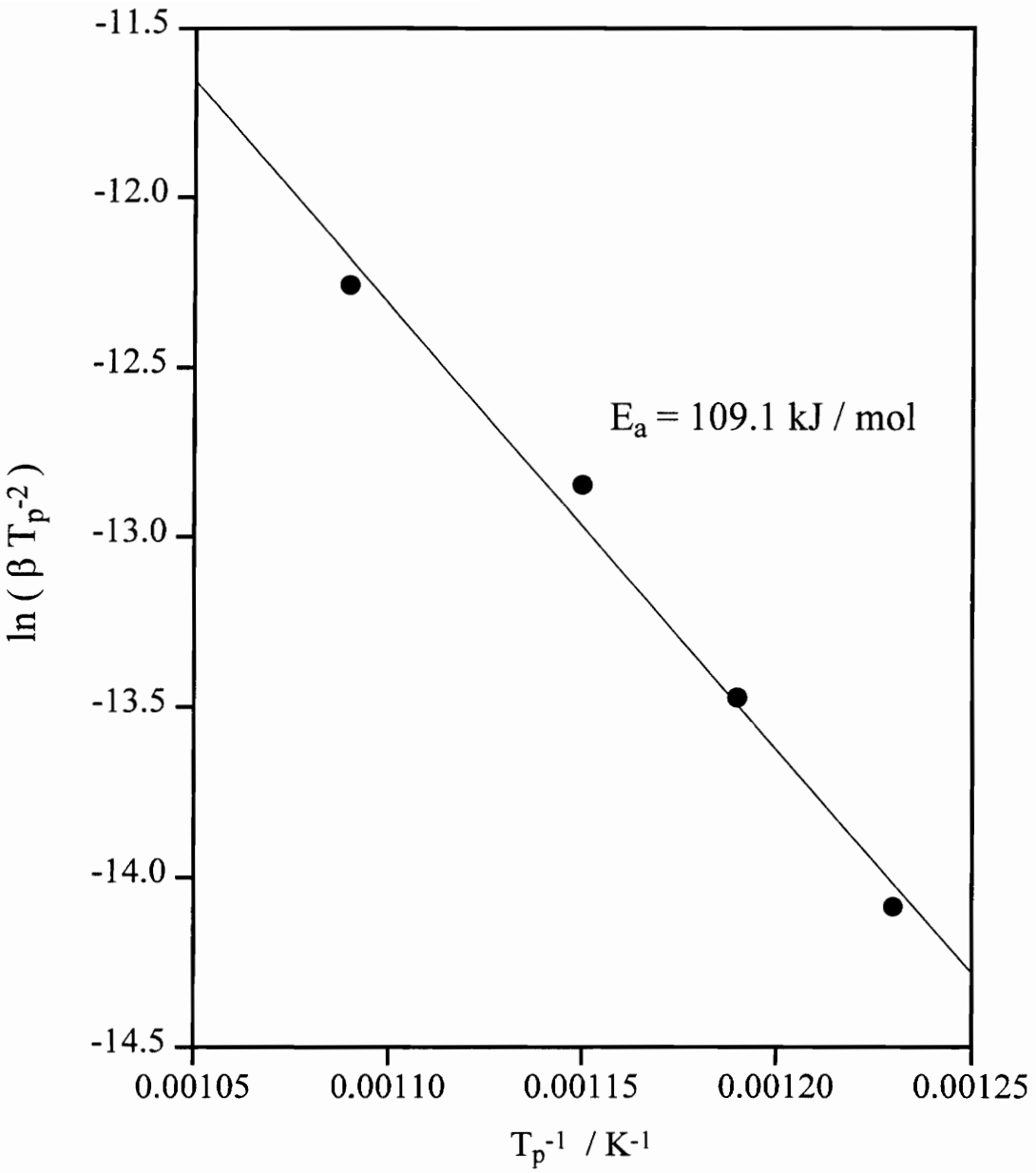

Figure 4: Results of Redhead Analysis for Determination of Activation Energy of Nitridation.

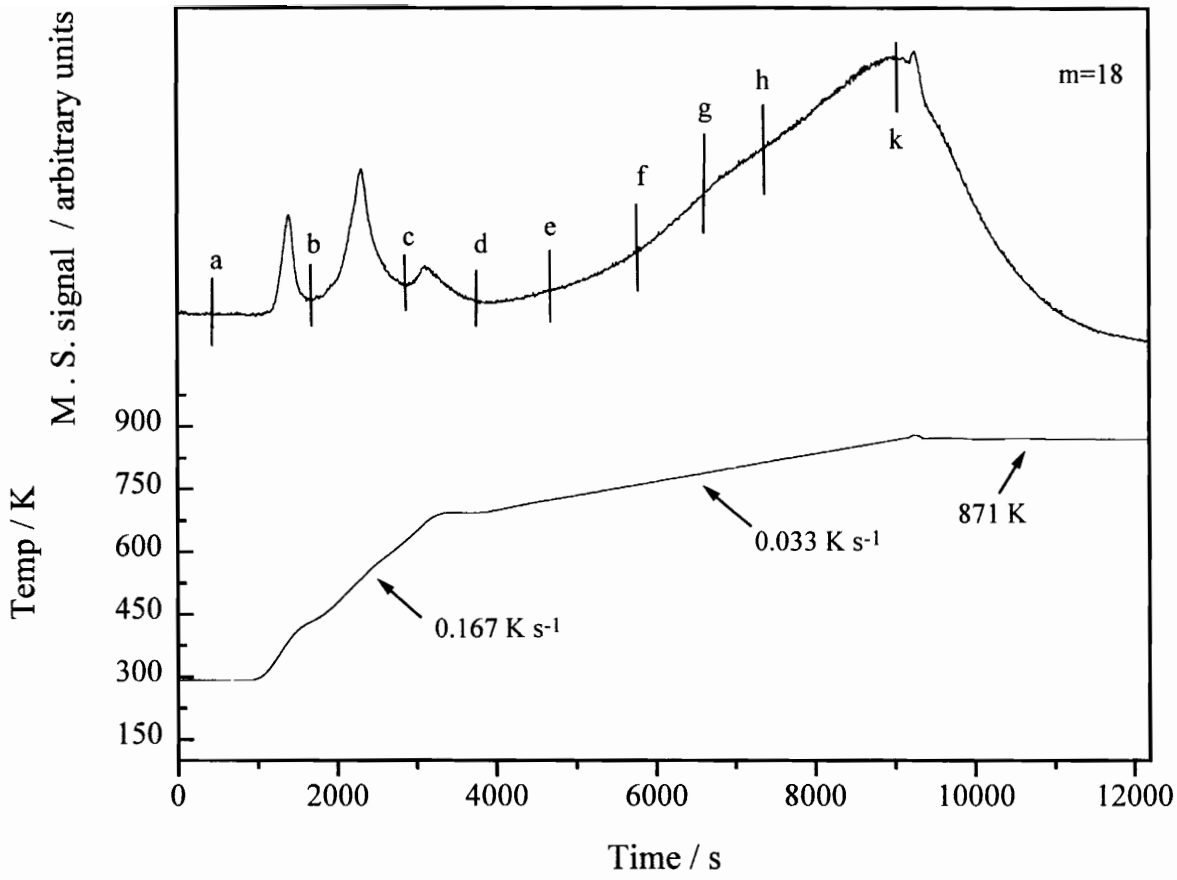

Figure 5: Mass Spectroscopy Trace of Mass 18 (H_2O) Showing Interruption Stages for Solid State Intermediate Study. A heating rate (β) of 0.033 K s^{-1} was used. The temperature program appears in the bottom portion of the figure.

4.2 **Characterization**

The identity of the final nitride product is in question. XRD results showed the absence of peaks associated with the WO_3 precursor. However, an fcc oxynitride phase of tungsten was found to have similar peak positions, intensities, and lattice parameter (a_o) as β-W_2N. The XRD patterns show lattice parameters that appear closer to the value for the oxynitride (a_o = 4.138 Å) in some of the samples, and closer to β-W_2N (a_o = 4.126 Å) in others. A qualitative elemental analysis conducted on two of the final product samples using an Electron Microprobe showed a substantial amount of oxygen present. A quantitative analysis of O and N weight percentages was conducted on one of the final product samples. Oxygen content was determined by heating the sample to 1100 K from ambient conditions in H_2 at a rate of 0.167 K s^{-1}, and monitoring the mass 18 (H_2O) signal with a mass spectrometer (Figure A6). In this way, the sample was reduced to tungsten metal. These results gave 10.6 wt. % O, and 5.4 wt. % N, the balance being W. This would give a stoichiometric formula of $WO_{1.5}N_{0.85}$. This compares to the chemical formula given by Kiessling and Peterson[19] of $W_{0.62}O_{0.38}N_{0.62}$ (which corresponds to $WO_{0.61}N$) that they reported in their study. The high oxygen content is partly due to chemisorption on the surface of these high surface area materials. An estimate of the amount of O_2 chemisorbed on the surface of this sample, using the number density of sites determined at 2.0×10^{17} m^{-2} by S_g and CO measurements, suggests that this contribution to the total amount of oxygen found in the sample is small (about 1 to 2

mol %). The oxygen content of the final product samples justifies the classification of the materials as oxynitrides.

Table 1 summarizes surface area (S_g) , CO uptake, site density, and crystallite size values obtained at different β. The crystallite sizes were determined by the Scherrer method of Equation 2. The trend shows a general increase in surface area with decreasing β. The value of 88 $m^2 g^{-1}$ obtained from 0.008 K s^{-1} shows close agreement with the value of 91 $m^2 g^{-1}$ determined by Volpe and Boudart[8] in their synthesis. The CO uptake results obtained do not show a definite increasing trend.

Table 1: Characterization results from use of different heating rates (β). Associated errors in values: $T_p \pm 5$ K, $S_g \pm 2$ $m^2 g^{-1}$, CO ± 2μmol g^{-1}, Dc ± 1 nm

β (K s^{-1})	T_p (K)	S_g ($m^2 g^{-1}$)	CO uptake (μmol g^{-1})	Site density (m^{-2}) / 1x10^{17}	Crystallite Size D_c / nm
0.008	810	88	64	4.4	12
0.017	842	87	110	7.6	11
0.033	871	72	62	5.2	12
0.067	918	71	40	3.4	14

From the data in Table 1, it seems that the optimal synthesis conditions for the oxynitride occur when a heating rate (β) of 0.017 K s^{-1} was employed. This resulted in the highest site density sample of the four that were studied. When a β of 0.008 K s^{-1} was used, the mass 18 peak was not as distinct as in the other samples, instead it appeared

more broad and flat in the traces. Due to the lack of a well defined sharp peak, the synthesis interruption occurred almost as a guess, even though the value of T_p was reproduced several times within a ten degree range around the value listed. The soak time duration at T_p was also hindered by the mass 18 signal, because it was not as clear that the peak had returned to baseline as it was when the other heating rates were used.

It was observed that several of the samples had a large reduction in measured surface area after storage for an extended period of time. Freshly prepared samples were measured to have a high S_g on the Micromeritics unit, if measured within a day or two of synthesis. However, if stored for several days then analyzed using the Micromeritics unit, the measured S_g would drop to values between 1-5 $m^2 g^{-1}$. Degassing these samples at 723 K for more than 2 h did not reproduce the original high S_g values. However, when the samples were reduced in 10% H_2/He at 723 K for 2 h on the synthesis unit, single point BET surface area values were restored to the initial high values. The Mass 18 mass spectroscopy signal recorded during reduction showed the evolution of water from the samples. This indicates that the loss of surface area is due to some slow oxidation process (possibly electrochemical) which oxidizes the surface and results in pore blockage. The values of S_g that appear in Table 1 are those obtained using the single point BET method.

The samples were characterized using XRD after the TPR runs. XRD patterns of all intermediate stages of synthesis are presented in Figures 6 and 7. The results show that the first mass 18 peak at 400 K is due to the reduction of the amount of the

$(NH_4)_{10}W_{12}O_{41}$ phase present in the sample (Figure 6 (b)). The tungstate phase might be represented as a hydrate of the following structure $(NH_3)_{10}\bullet W_{12}O_{36}\bullet(H_2O)_5$. This would explain the mass 18 peak at 400K, as well as a simultaneous mass 30 peak that was often noticed. The second mass 18 peak at 560 K is due to the removal of the $(NH_4)_{10}W_{12}O_{41}$ phase, leaving only the triclinic WO_3 phase originally present in the precursor powder (Figure 6 (c)). The third mass 18 peak at 670 K shows the formation of a hexagonal WO_3 phase in addition to the triclinic form of the original powder (Figure 6 (d)). Mass 30 peaks corresponding to NO also occurred simultaneously with the first two mass 18 peaks, which supports the removal of the $(NH_4)_{10}W_{12}O_{41}$ phase. In experiments in which it was actually possible to use the WO_3 powder as received, the three lower temperature mass 18 peaks were not observed (Figure A4). The use of XRD also showed that there was no formation of the hexagonal WO_3 upon heating of the triclinic powder (Figure A5). These results further indicate that the stages of reaction just described were due solely to the removal of the ammonium tungstate phase from the pellets that were formed.

Next, samples (e) through (k), occurring along the higher temperature mass 18 peak in Figure 5 were studied. XRD results taken on these samples indicated no distinct formation of intermediates along the synthesis path. The XRD patterns do show that the hexagonal phase WO_3 is gradually removed from the sample until at 813 K (Figure 7 (h)) it is nearly gone. In addition, a monoclinic $WO_{2.9}$ phase was seen in samples (e) through (h). This suboxide was also seen, with XRD, when the triclinic WO_3 powder was heated to 813 K (Figure A5). This confirmed that the addition of ammonium hydroxide was not

the cause of the formation of this suboxide. The fcc oxynitride began to first appear in sample (f). At 873 K (Figure 7 (k)) the sample is fully converted to the fcc oxynitride. The possibility exists that the triclinic WO_3 underwent a continuous transformation in becoming the oxynitride product, with no other distinct individual phases formed. This is similar to the results obtained by Volpe and Boudart[8] in their synthesis of Mo_2N using the MoO_3 / NH_3 reaction. CO uptake, S_g analysis, and nitrogen content elemental analysis were also carried out on these samples (Table 2). The results show a clear increase in surface area and CO uptake as the synthesis proceeds towards T_p. These results are plotted in Figure 8. Table 2 also shows a definite increase in the amount of nitrogen being incorporated into the samples as the reaction proceeds towards completion. These results are plotted in Figure 9.

Table 2: Characterization of Samples (a), and (e) through (k) from Figure 5. The data demonstrate formation of surface area, increase in CO uptake, and increase in wt. % nitrogen content. Surface areas were measured by single point BET method. Associated errors: $T_p \pm 5$ K, $S_g \pm 2$ $m^2 g^{-1}$, CO $\pm$ 2μmol g^{-1}, N content $\pm$ 0.3 %

Sample	T_{max} (K)	S_g ($m^2 g^{-1}$)	CO uptake (μmol g^{-1})	Site density (m^{-2}) / $1x10^{17}$	Nitrogen content wt. %
a	298	3	1	2	0.0
e	723	6	0	0	3.1
f	763	23	10	2.6	3.5
g	788	28	13	2.8	3.8
h	813	48	22	2.8	4.5
k	871	71	62	5.3	5.4

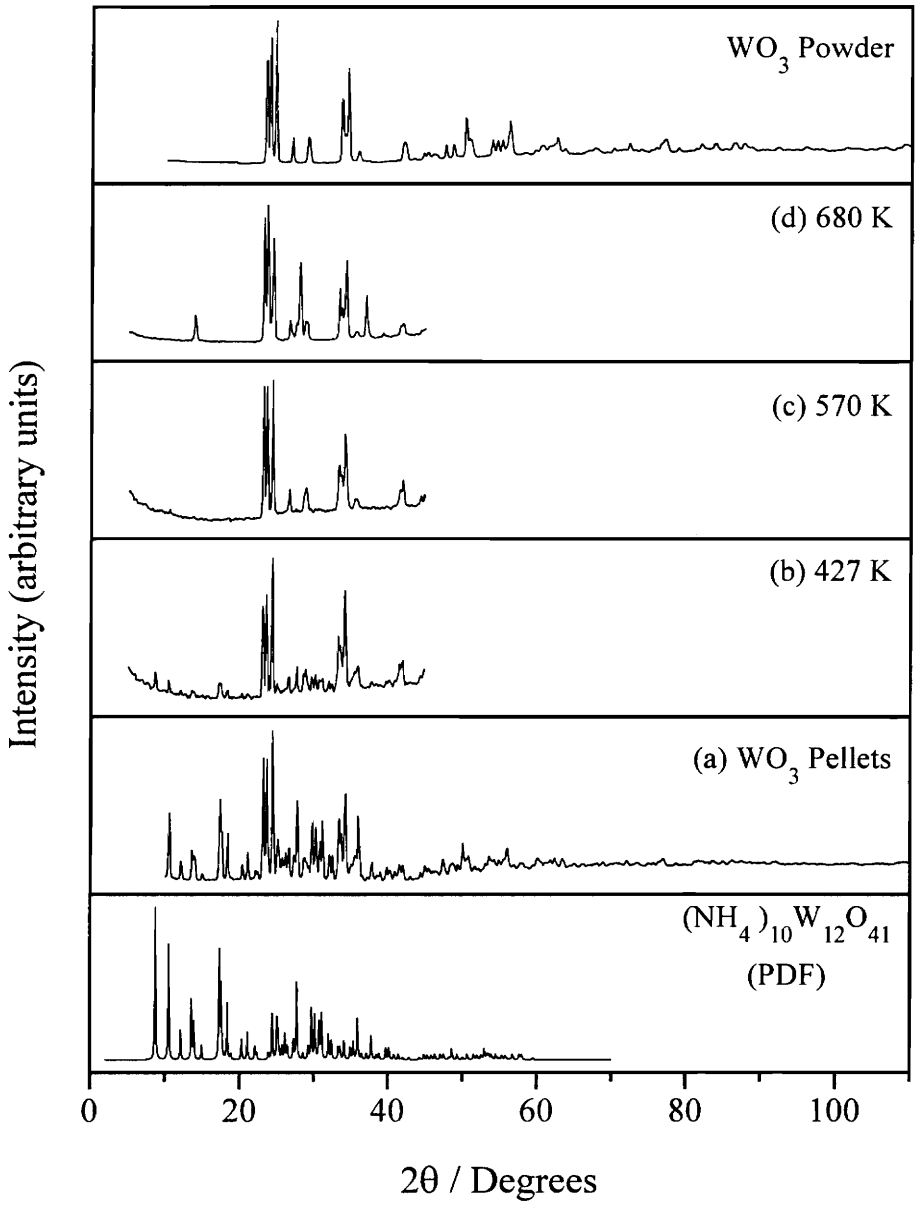

Figure 6: XRD Patterns for the Interrupted Stages Appearing in Figure 5. Successive stages show removal of ammonium tungstate phase from the sample to recover single phase WO_3, as well as the formation of a hexagonal phase WO_3. The WO_3 pellets were formed by addition of ammonium hydroxide to WO_3 powder.

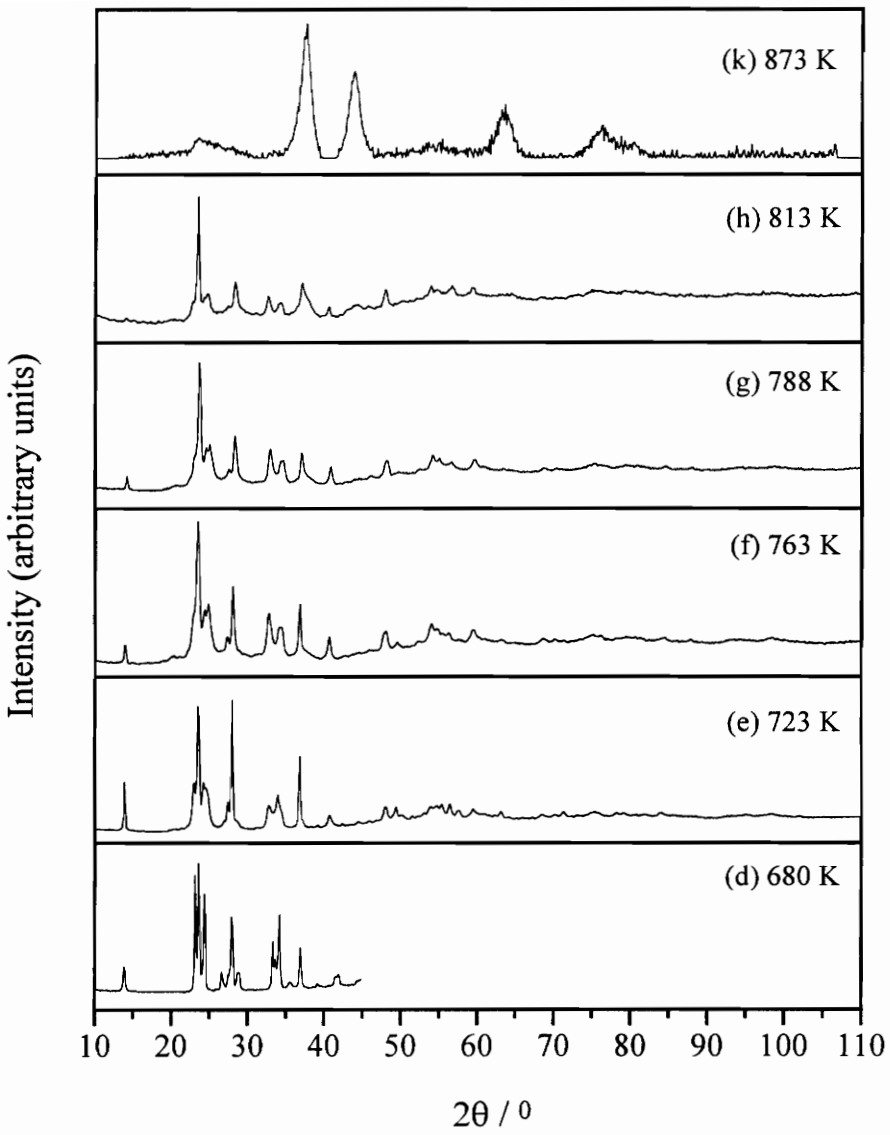

Figure 7: More XRD Patterns for Interrupted Stages Appearing in Figure 5. The patterns show no well defined solid-state intermediates along the synthesis path. The hexagonal phase of WO_3 disappears from the traces at 813 K. Sample (k) at 873 K, corresponding to T_p, represents the final oxynitride product.

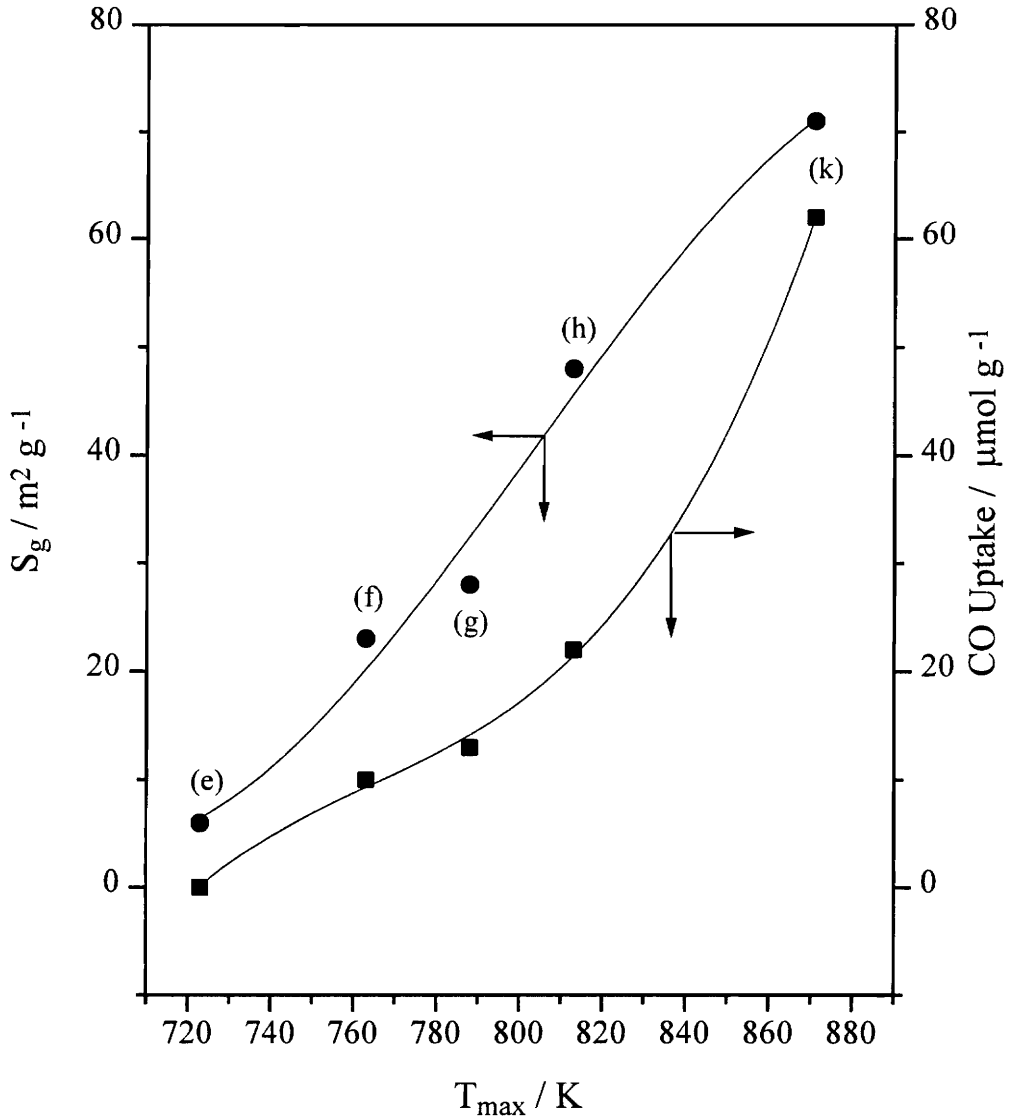

Figure 8: Graphical Representation of Formation of Surface Area and Increase in CO Uptake for Samples (e) through (k) Appearing in Figure 5. The data for surface area (in m^2 g^{-1}) appear as circles, while the CO uptake values (in μmol g^{-1}) appear as squares. The two curved lines show the general trend of the data.

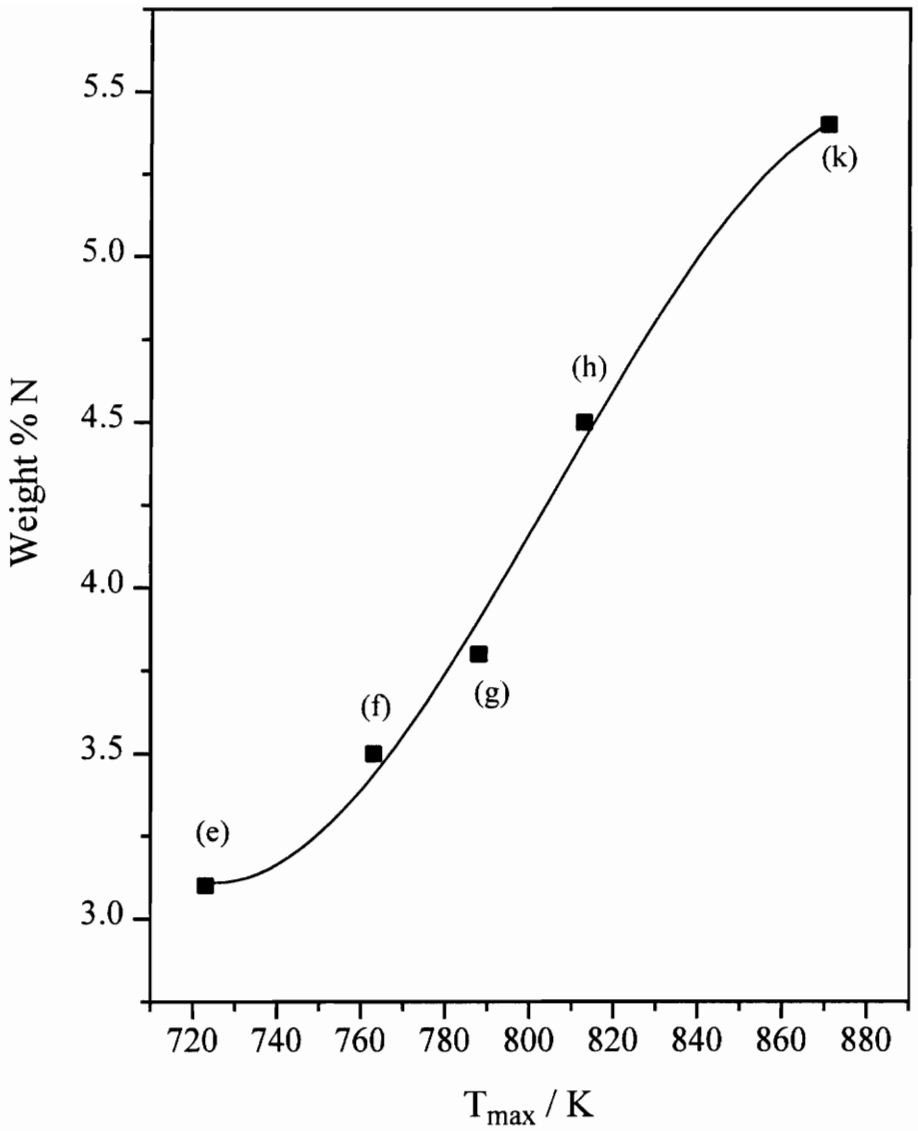

Figure 9: Graphical Illustration Showing Increase in Nitrogen Content in Samples (e) through (k) Appearing in Figure 5. The curved line shows the general trend of the data.

4.3 **Reactivity**

The activity of tungsten oxynitride showed some interesting results in the three reactivity experiments studied. Previous reactivity experiments using β-W_2N as a catalyst have also been conducted. These include the hydrotreating of quinoline and thiophene[12], the dehydration of 2-octanol as well as the conversion of 2-octylamine[14]. Tungsten oxynitride compounds have also been studied for n-heptane isomerization[13]. In the hydroprocessing experiment the catalyst seemed to show a steady hydrogenation activity (% HYD) of about 40 % through the experiment. However, this activity was in fact due to non-catalytic hydrogenation of the quinoline as it passed through the quartz chips in the reactor bed. This result has been seen previously in a number of similar experiments performed using the same trickle-bed reactor[9].

Therefore, the catalytic hydrogenation of quinoline reported here is actually negligible. This is in contrast to the results obtained by Abe, Cheung and Bell, who reported a fair amount of quinoline hydrogenation activity for β-W_2N[12]. The % HDO activity rose to about 15 % after 15 h on-line, and then held steady at this value. The % HDS activity initially started out at about 25 %, but then declined quickly after about 17 h on-line, until it finally stabilized at around 5 %. The % HDN activity mirrored the % HDS, initially at about 5 % until 17 h on-line at which point it rose rapidly until stabilizing at about 20 %. These results are shown in Figure 10.

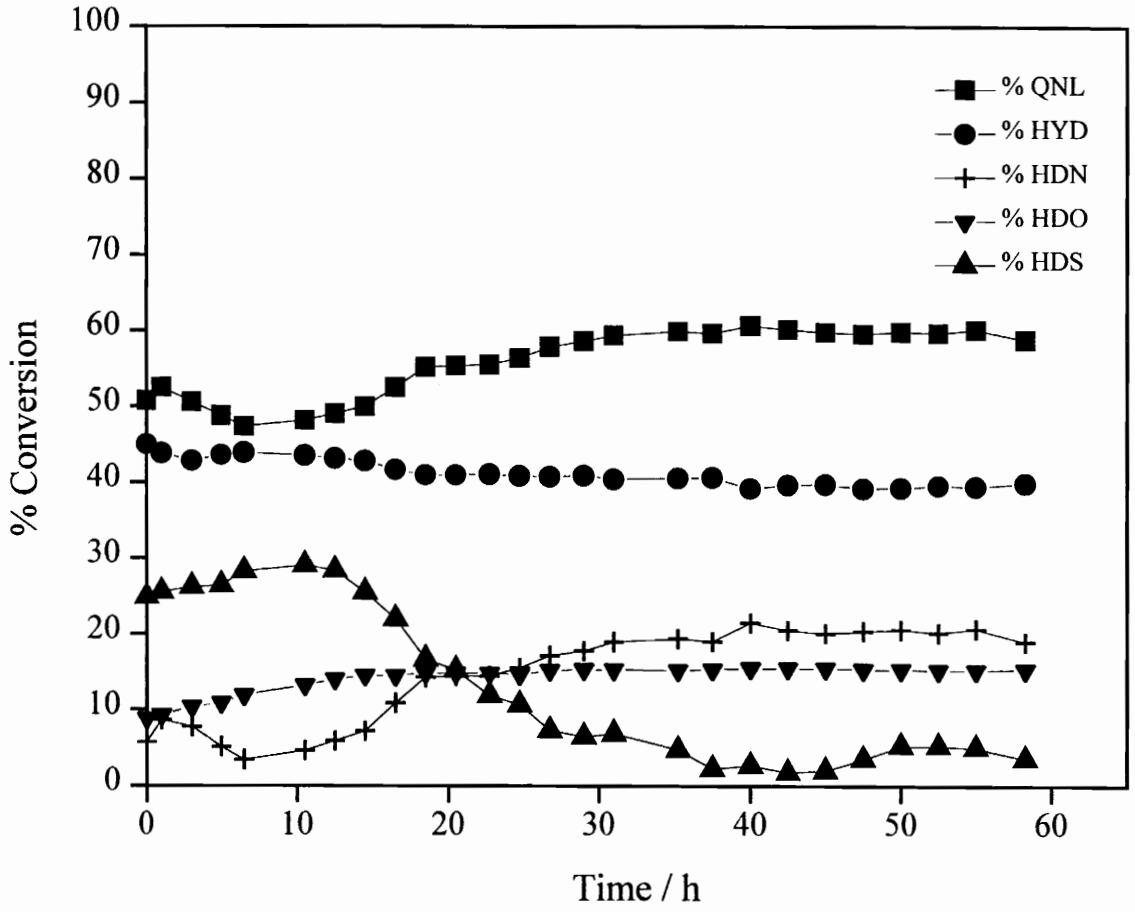

Figure 10: Activities for the Hydroprocessing Reactivity Experiment as a Function of Time On-line.

On examining the quinoline HDN product distribution, it seems that tungsten oxynitride compared reasonably well with the other catalysts investigated by Ramanathan and Oyama[9]. Table 3 shows the product distribution that results from the conversion of quinoline using these catalysts. The results for tungsten oxynitride can be found at the bottom of this table. The products are all in mol %. For an explanation of the abbreviations used for the products see the proposed reaction network diagram in Figure A2 of the Appendix.

Table 3: Comparison of Product Distributions for Several Carbides / Nitrides[9]. The values obtained for tungsten oxynitride appear in the last row. The products appearing in the table all have values of mol %. The column labeled others represents light hydrocarbons and gaseous products. Explanation of the product abbreviations appears in Figure A2 of the Appendix.

Catalyst	QNL conv. / %	1-THQ	5-THQ	OPA	PCH	PBZ	Others
Ni-Mo/Al_2O_3	85	20	30	6	23	12	9
Mo_2C	86	14	24	6	30	11	15
WC	81	21	36	5	10	7	20
NbC	57	89					11
VC	44	82	14				4
Mo_2N	73	24	40	6	8	8	15
TiN	43	67	28				5
VN	66	55	36				9
WO_xN_y	53	26	34	6	3	3	28

A comparison can be made between the tungsten oxynitride used, and the carbides and nitrides that were used by Ramanathan and Oyama in their study. First of all, the HDO activity of tungsten oxynitride was only surpassed by VN and the commercial sulfided Ni-Mo catalyst. The HDN activity of the oxynitride was also fairly good, exceeding the values obtained by NbC, VN, VC, and TiN, and equaling the value for Mo_2N. A comparison of HDN activities for various nitrides appears in Figure 11. For HDS activity, the oxynitride did not perform very well, having percentages close to those obtained for NbC, VN, VC, and TiN. The oxynitride also seems to be producing a number of cracked products which would appear in the form of light hydrocarbons or gases. This appears in Table 3 under the heading of others, and makes up about 28 % of the total number of product moles formed. If the reaction network that appears in Figure A2 is valid, then this would suggest that a large portion of the products that become propylcyclohexane (PCH) or propylbenzene (PBZ) undergo cleavage of carbon bonds to form these light hydrocarbons and gaseous products. These products are difficult to analyze with gas chromatography, due to overlap of retention times, and therefore no discussion of their composition or mol % amounts will appear in this report.

The cumene hydrogenation experiment showed that there was essentially no hydrogenation of the benzene ring to form isopropylcyclohexane. This result suggests that the catalyst does not show good activity for hydrogenation of aromatic compounds. The possibility exists that cumene is sterically hindered from moving parallel, and close,

to the surface, which would prevent the benzene ring from becoming hydrogenated. To check further for possible hydrogenation, another test molecule, styrene, was studied.

In the styrene hydrogenation experiment, initial results showed the selective hydrogenation of the ethenyl group to form ethylbenzene, with very little hydrogenation of the benzene ring to form ethylcyclohexane. A steady-state conversion of about 95% styrene to ethylbenzene was observed. However, this turned out to be a negative result as the hydrogenation to ethylbenzene seemed to be occurring by non-catalytic gas phase reaction. Addition of 100 ppm dibenzothiophene reduced the hydrogenation activity to form ethylcyclohexane to essentially 0 %, while it did not alter the hydrogenation to form ethylbenzene at all. This experiment also would seem to confirm the results of the cumene experiment, in that tungsten oxynitride does not act as a good hydrogenation catalyst for aromatics.

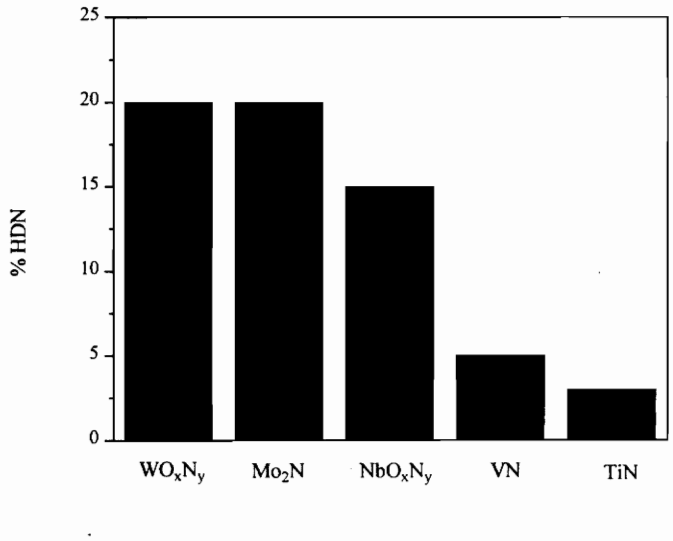

Figure 11: Comparison of HDN Activities for various Nitrides.

5. Conclusions

The TPR synthesis method employed produced a tungsten oxynitride phase of high surface area. The formation of an oxynitride is probably due to the temperatures at which the experiments were halted, and then soaked at. It appears that it would be difficult to form a pure phase β-W_2N using elevated temperatures without forming a metal phase, as was found to occur in the initial synthesis attempts of this investigation. The production of a pure phase β-W_2N does however warrant further investigation. In-situ characterization techniques would determine whether the nitride is actually formed by the TPR synthesis, and then an oxynitride formed when the samples are passivated in O_2. It might also be possible to form pure phase β-W_2N by nitriding for prolonged periods at low temperatures.

Additionally, the formation of WO_xN_y from WO_3 has been well characterized here. Changes in crystal structure, surface area, CO chemisorption, and nitrogen content along the synthesis path have all been established. These results will prove useful in further studies concerning WO_xN_y synthesis.

The oxynitrides that were prepared in this study show many positive aspects when compared to the pure β-W_2N. In terms of characterization, the oxynitrides have been shown to have high surface areas, equivalent to values obtained for the pure nitride. Also, relatively good values of CO chemisorption were obtained for the oxynitrides. In addition, the oxynitrides have been shown to have a lower activation energy for nitridation than was previously reported which makes their synthesis more favorable.

The three reactivity studies conducted here have shown some mixed results, however as to the catalytic benefits of these oxynitrides. It appears from these separate reactivity experiments that the oxynitrides are not good hydrogenation catalysts, especially where aromatics are concerned. The HDS activity that initially seemed promising, also dropped considerably during the course of the hydroprocessing experiment. This seems to suggest that sulfur removal from liquid feeds by tungsten oxynitrides is not practically feasible. They do, however, maintain respectable HDN and HDO activities over the course of 60 h on line. A further study should examine the surface characteristics of the samples following reactivity experiments, possibly by the use of XPS. Coupled with the potential for low synthesis cost, these HDN and HDO activities show that the oxynitrides of tungsten deserve further investigation.

6. Appendix

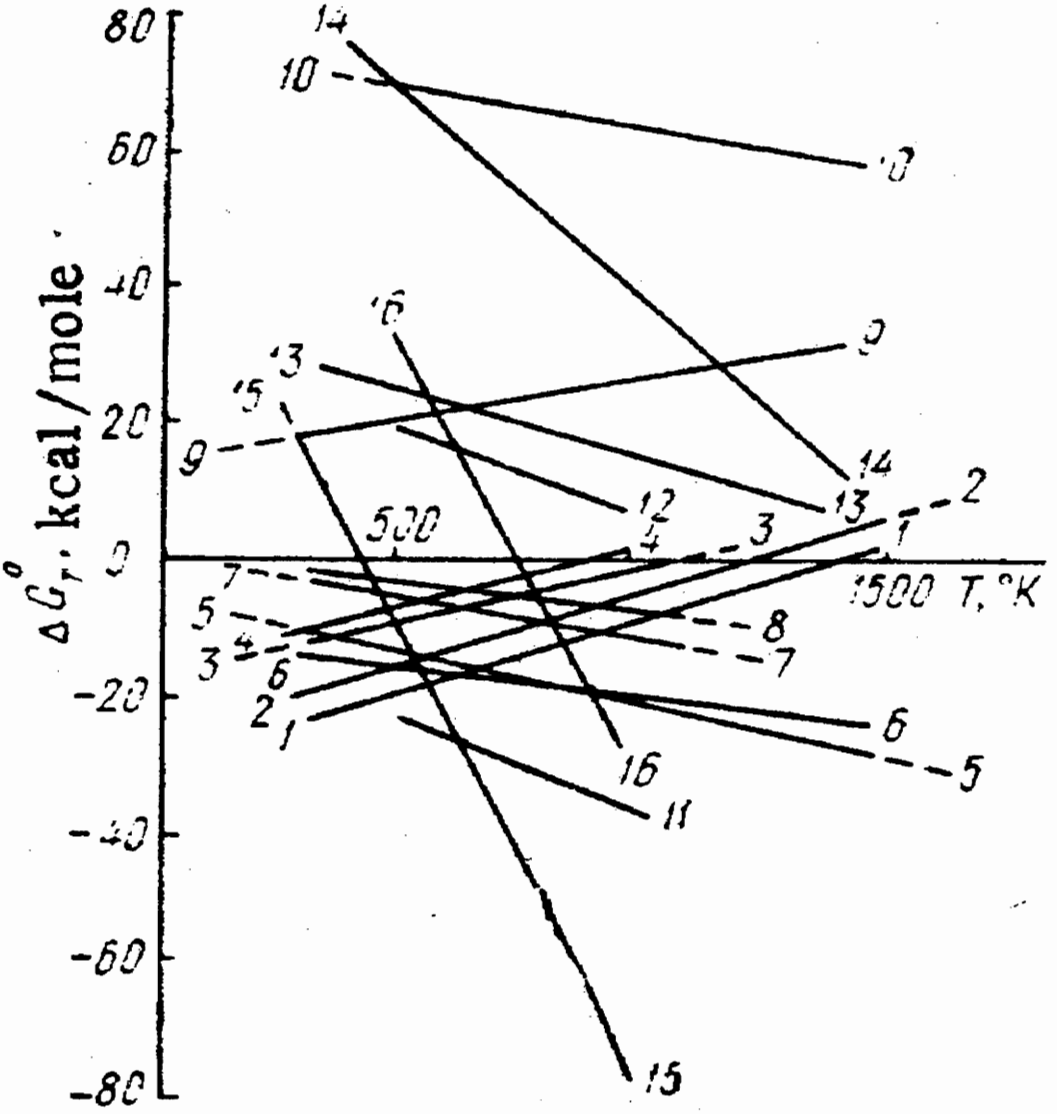

Figure A1: Effect of temperature on isobaric-isothermal potentials of formation of Group VIA nitrides in reactions: 1) $Cr + ½N_2 \rightarrow CrN$; 2) $2Cr + ½N_2 \rightarrow Cr_2N$; 3) $2Mo + ½N_2 \rightarrow Mo_2N$; 4) $2W + ½N_2 \rightarrow W_2N$; 5) $Cr + NH_3 \rightarrow CrN + 3/2H_2$; 6) $2Cr + NH_3 \rightarrow Cr_2N + 3/2H_2$; 7) $2Mo + NH_3 \rightarrow Mo_2N + 3/2H_2$; 8) $2W + NH_3 \rightarrow W_2N + 3/2H_2$; 9) $½\ Cr_2O_3 + 3/2H_2 + ½N_2 \rightarrow CrN + 3/2H_2O$; 10) $Cr_2O_3 + 3H_2 + ½N_2 \rightarrow Cr_2N + 3H_2O$; 11) $2MoO_3 + 6H_2 + ½N_2 \rightarrow Mo_2N + 6H_2O$; 12) $2WO_3 + 6H_2 + ½N_2 \rightarrow W_2N + 6H_2O$; 13) $½\ Cr_2O_3 + NH_3 \rightarrow CrN + 3/2H_2O$; 14) $Cr_2O_3 + 2NH_3 \rightarrow Cr_2N + 3H_2O + ½N_2$; 15) $2MoO_3 + 4\ NH_3 \rightarrow Mo_2N + 6H_2O + 3/2N_2$; 16) $2WO_3 + 4NH_3 \rightarrow W_2N + 6H_2O + 3/2N_2$

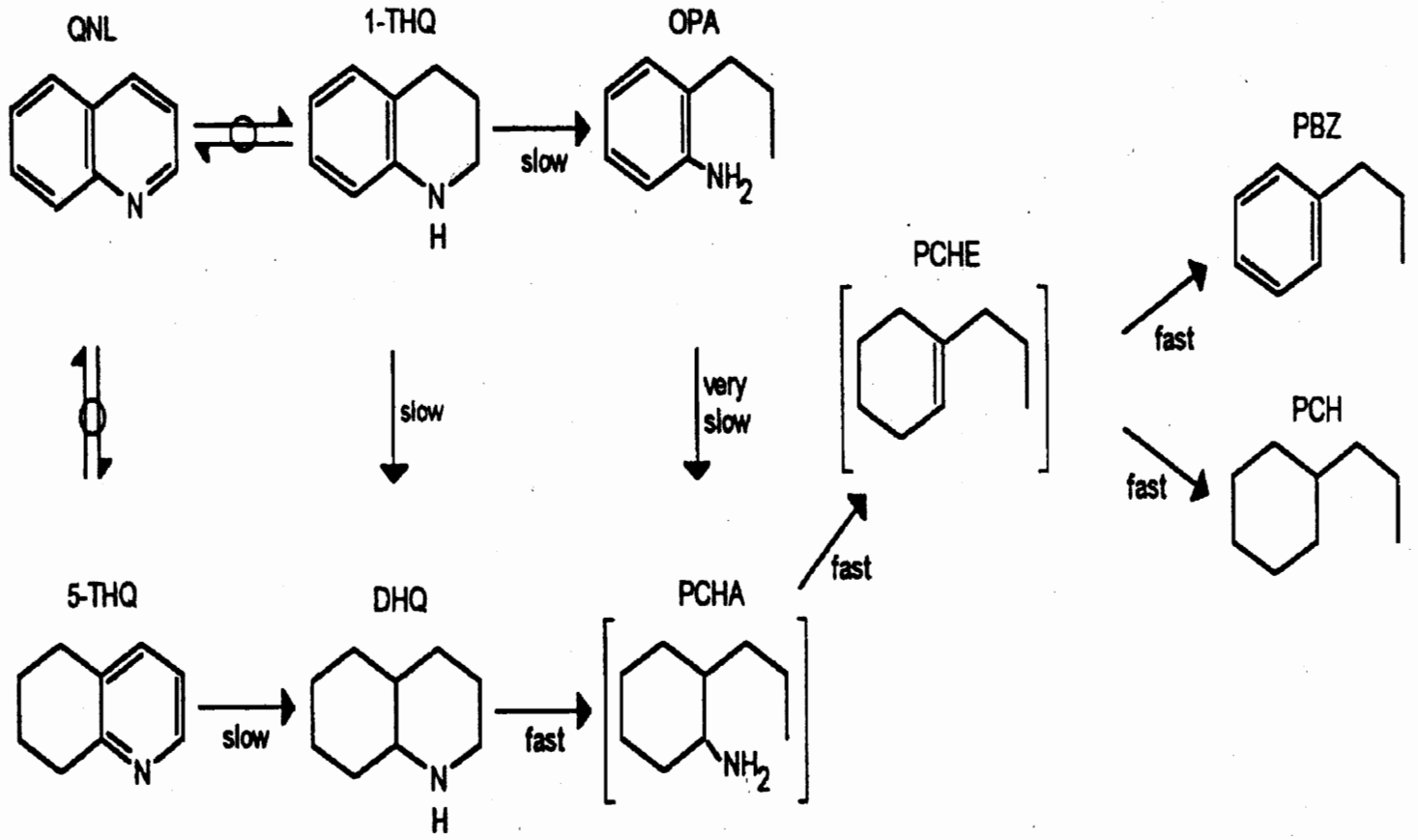

Figure A2: Proposed reaction pathway products for quinoline hydrodenitrogenation[9]: QNL, quinoline; 1-THQ, 1,2,3,4-tetrahydroquinoline; 5-THQ, 5,6,7,8-tetrahydroquinoline; DHQ, decahydroquinoline; OPA, *o*-propylaniline; PCHA, propylcyclohexylamine; PCHE, propylcyclohexane; PBZ, propylbenzene; PCH, propylcyclohexane.

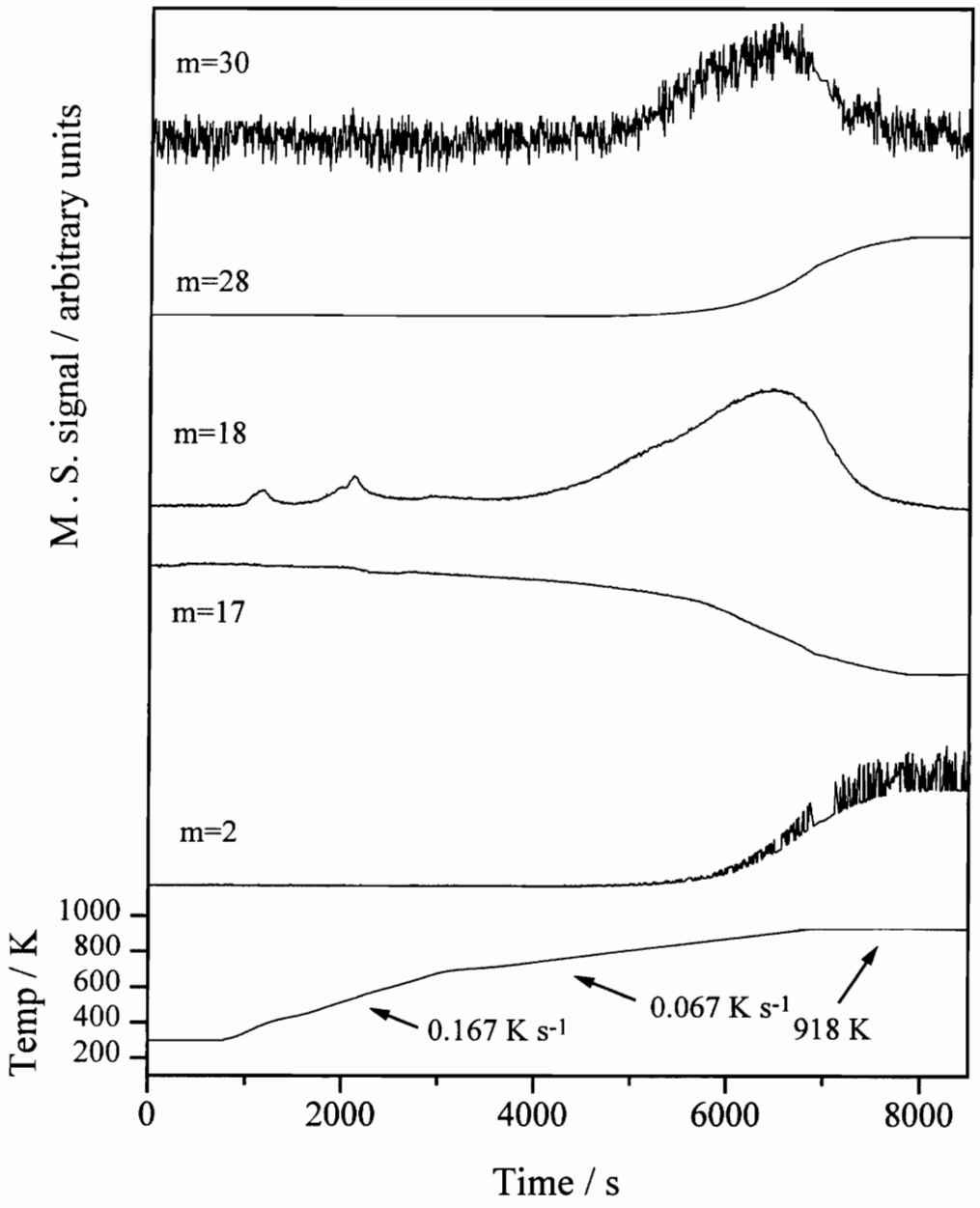

Figure A3: Representative TPR Synthesis of WO_xN_y from WO_3 pellets prepared. Mass Signals: 2 (H_2), 17 (NH_3), 18 (H_2O), 28 (N_2), and 30 (NO) are shown. There are actually three lower temperature mass 18 peaks, but only two are distinguishable here.

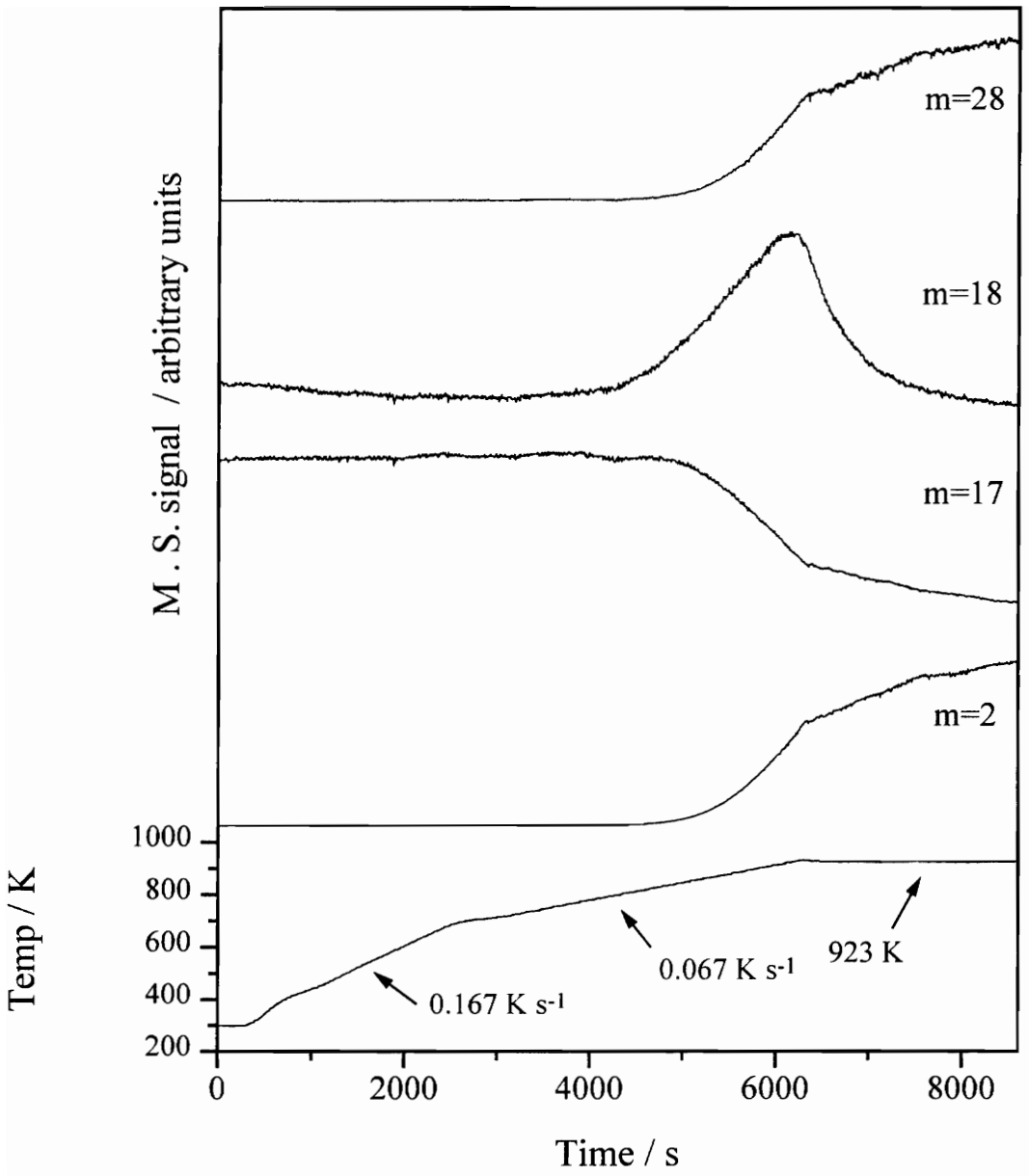

Figure A4: TPR Synthesis of WO_xN_y from WO_3 powder. Mass Signals: 2 (H_2), 17 (NH_3), 18 (H_2O), and 28 (N_2) are shown. Note absence of low temperature mass 18 peaks.

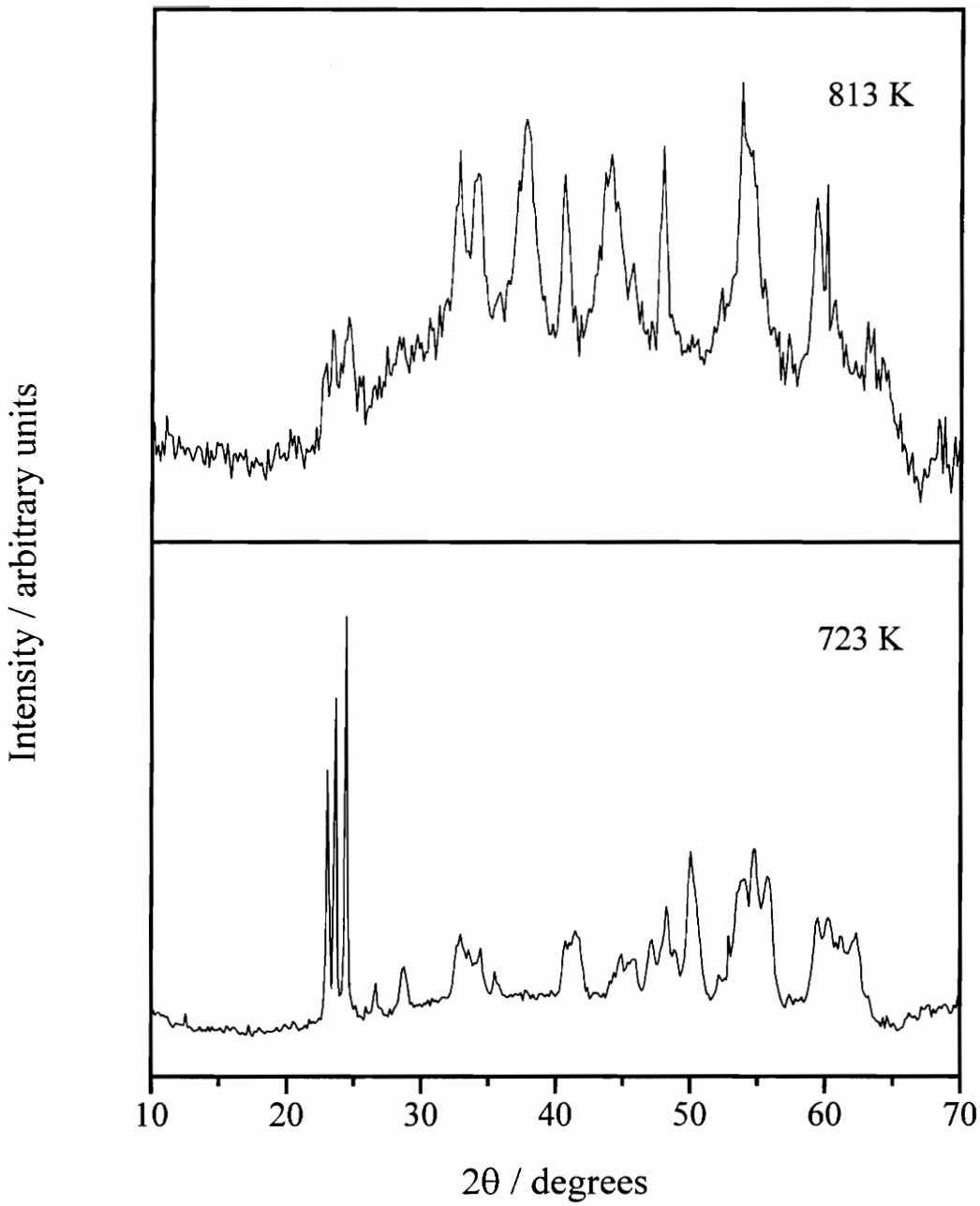

Figure A5: XRD Patterns of Interrupted Synthesis Samples Prepared Using WO_3 Powder. The results at 723 K show that no formation of a hexagonal WO_3 phase as was found using the WO_3 pellets. The results at 813 K show the formation of a monoclinic $WO_{2.9}$ phase, identical to the results obtained with the WO_3 pellets.

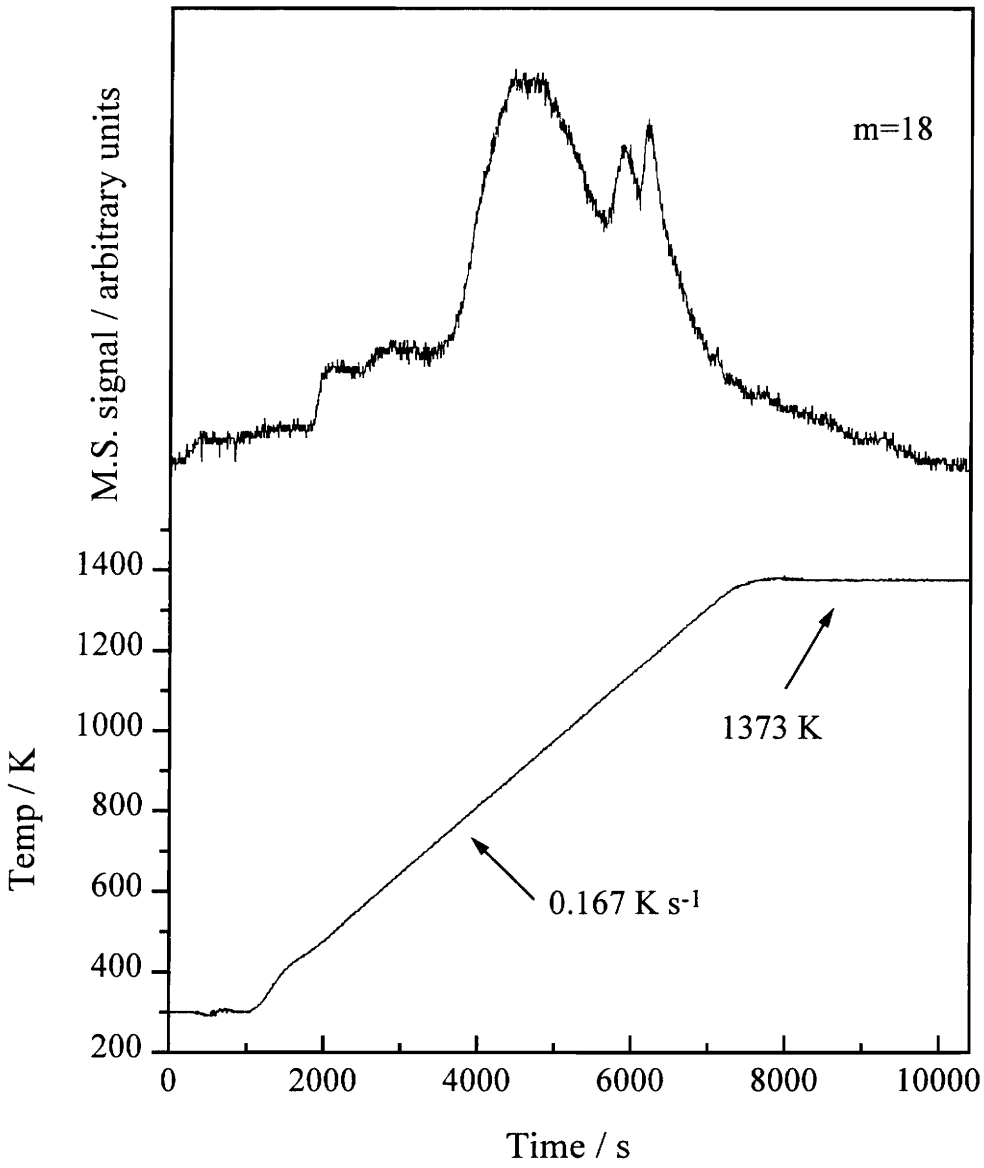

Figure A6: Decomposition of WO_xN_y in H_2 to Determine Oxygen Weight Content. Mass 18 (H_2O) signal is presented, and was the only signal found for oxygen release from the sample. The oxygen content determined was 10.6 % by weight. Temperature program is shown at bottom.

7. References

[1] L. E. Toth, "Transition Metal Carbides and Nitrides", New York, Academic Press, 1967.

[2] A. Bosseboeuf, A. Fourrier, F. Meyer, A. Benhocine, and G. Gautherin, *Appl. Surf. Sci.* 53 (1991) 353.

[3] S. Ted Oyama, Editor, "The Chemistry of Transition Metal Carbides and Nitrides", Chapter 1, Blackie Academic & Professional, London, 1996.

[4] G. Hägg, *Z. Phys. Chem.*, 12 (1931) 33.

[5] L. Brewer, *Science*, 161 (1968) 115.

[6] P. Schwartzkopf and R. Kieffer, "Refractory Hard Metals", Macmillan, New York, 1953.

[7] S. T. Oyama, Ph.D. Dissertation, Stanford University, 1981.

[8] L. Volpe and M. Boudart, *J. Solid State Chem.*, 59 (1985) 332.

[9] S. Ramanathan and S. T. Oyama, *J.Phys. Chem.*, 99 (1995) 16365.

[10] B. Dhandapani and S. T. Oyama, *Catal. Lett.*, 35 (1995) 353.

[11] J. S. Lee, M. H. Yeom, K. Y. Park, I.-S. Nam, J. S. Chung, T. G. Kim, and S. H. Moon, *J. Catal.*, 128 (1991) 126.

[12] H. Abe, T-k. Cheung, and A. T. Bell, *Catal. Lett.*, 21 (1993) 11.

[13] S. Sellem, C. Potvin, J. M. Manoli, R. Contant, and G. Djéga-Mariadassou, *J. Chem. Soc., Chem. Comm.*, 3 (1995) 359.

[14] J. H. Lee, C. E. Hamrin, Jr., and B. H. Davis, *Catal. Today*, 15 (1992) 223.

[15] T. Ya Kosolapova, "Carbides, Properties, Production, and Applications", Plenum Press, New York, 1971

[16] S. T. Oyama, In: "Handbook of Heterogeneous Catalysis", G. Ertl, H. Knözinger, J. Weitkamp, Eds, (VCH, Weinheim), In press

[17] I. I. Zhukov, Izv. Sektora Fiz. -Khim. Anal. Akad. Nauk SSSR, 3, (1926), 14

[18] M. D. Lyutaya, Translated from *Poroshkovaya Metallurgiya*, 3 (195), (1979), 60

[19] R. Kiessling, L Peterson, *Acta Metallurgica*, 2, (1954), 675

[20] F. Benesovsky, R. Kieffer and P. Ettmayer, *Nitrides* In: *Kirk Othmer, Encyclopedia of Chemical Technology*, 3rd edition, Vol. 15 (John Wiley & Sons, New York, 1981), 871

[21] J.S. Haggerty. In: *Laser Induced Chemical Processes*, J.I. Steinfeld, Ed., (Plenum Press, New York, 1981)

[22] X.-X. Bi, B. Ganguli, G.P. Huffman, F.E. Huggins, M. Endo and P.C. Eklund, *J. Mater. Res.*, 8, (1993), 1666

[23] X.-X. Bi, K. D. Chowdhury, W. T. Lee, S. Bandow, M. S. Dresselhaus, and P. C. Eklund, *Mat. Res. Soc. Symp. Proc.*, 368, (1995), 69

[24] J. S. Lee, S.T. Oyama, and M. Boudart, *J. Catalysis*, 106, (1987), 125

[25] P. Ho, R. J. Buss and R.E. Loehman, *J. Mater. Res.*, 4, (1989), 873

[26] S. Dressler, *Indust. Heating*, 38, December (1991)

[27] D. Pye, *Indust. Heating*, 33, January (1992)

[28] C. F. Powell, J.H. Oxley, and J. M. Blocker, *Vapor Deposition*, (Wiley, New York, 1966)

[29] D. P. Stinton, T. M. Bessman, and R. A. Lowden, *Am. Ceram. Soc. Bull.*, 67, (1988), 350

[30] M. Podob, *Indust. Heating*, 23, December (1992)

[31] G. S. Girolami, and J. E. Gozum, *Mat. Res. Soc. Symp. Proc.*, 168, (1990), 319

[32] M. Nagai, and K. Kishida, *Applied Surface Science*, 70/71, (1993), 759

[33] A. Bosseboeuf, A. Fourrier, F. Meyer, A. Benhocine, and G. Gautherin, *Applied Surface Science*, 53, (1991), 353

[34] G. Weiss, *Ann. Chim.*, 1, (1946), 424, 446

[35] L. Andrieux, and G. Weiss, *Bull. Soc. Chim. France*, 15, (1948), 598

[36] M. Nagai, and T. Miyao, *Catal. Lett.*, 18, (1993), 9

[37] K. S. Lee, H. Abe, J. A. Reimer, and A. T. Bell, *J. Catalysis*, 139, (1993), 34

[38] J. C. Schlatter, S. T. Oyama, J. E. Metcalfe, III, and J. M. Lambert, Jr., *Ind. Eng. Chem. Res.*, 27, (1988), 1648

[39] J. S. Lee, and M. Boudart, *Applied Catalysis*, 19, (1983), 207

[40] E. J. Markel, and J. W. Van Zee, *J. Catalysis*, 126, (1990), 643

[41] I. Kojima, E. Miyazaki, Y. Inoue, and I. Yasumori, *J. Catalysis*, 73, (1982), 128

[42] B. Vidick, J. Lemaitre, and L. Leclercq, *J. Catalysis*, 99, (1986), 439

[43] M. Boudart, S. Locatellli, J. S. Lee, and S. T. Oyama, *J. Catalysis*, 125, (1990), 157

[44] F. H. Ribeiro, M. Boudart, R. A. Dalla Betta, and E. Iglesia, *J. Catalysis*, 130, (1991), 498

[45] M. J. Ledoux, C. Pham Huu, J. Guille, and H. Dunlop, *J. Catalysis*, 134, (1992), 383

[46] F. H. Ribeiro, R. A. Dalla Betta, M. Boudart, J. Baumgartner, and E. Iglesia, *J. Catalysis*, 130, (1991), 86

[47] P. A. Redhead, *Vacuum*, 12, (1962), 203

[48] B. D. Cullity, Chapter 3, "Elements of X-Ray Diffraction", 2nd Edition, Addison-Wesley Publishing Co., Inc., 1978

[49] R. Kapoor, S. T. Oyama, *J. Solid State Chem.*, 99, (1992), 303